FMH606 Master's Thesis 2024

Energy and Environmental Technology

Structural Loads Due to Detonations in Hydrogen Emergency Vent Systems

Rukon Ahmed Eimon

Faculty of Technology, Natural Sciences and Maritime Sciences
Campus Porsgrunn

University of
South-Eastern Norway

Course: FMH606 Master's Thesis, 2024

Title: Structural Loads Due to Detonations in Hydrogen Emergency Vent Systems

Number of pages: 70

Keywords: DDT, Shock Wave, run-up distance, Overpressure, Equivalence Ratio, Strain

Student:	Rukon Ahmed Eimon
Supervisor:	Dag Bjerketvedt and Magne Bratland
External partner:	Equinor

Summary:

Hydrogen emergency vent systems are safety equipment to release hydrogen from storage in terms of pressure rise. Sometimes, the safety vent systems become a risk when it fails, and several explosions happened due to this failure. In this study, hydrogen explosions at different concentrations were conducted in a 4 m single obstructed closed pipe to observe the maximum pressure and strain response. PicoSope and NI instruments were used to measure the pressure and strain respectively and it was found that NI recorded a lot of noise. No detonation or DDT was observed at $\varphi = 0.6$, but DDT was observed after the obstacle at $\varphi = 1.0$ and 1.2. The run-up distance was minimum in stoichiometric and rich mixtures. Maximum overpressure was observed as 1.85 MPa at 1.5 m distance at $\varphi = 1.2$. DDT was observed in end pipe at $\varphi = 0.8$ with a maximum reflected overpressure of 2.56 MPa. A DDT in the end pipe is dangerous and can develop a pressure of 5 MPa or even more. A dynamic amplification factor of 1.67 was found between the hoop strain recorded from strain gauge and strain calculated from internal pressure at 2.0 m distance for $\varphi = 1.0$. A random choice numerical simulation was conducted and compared with experimental results which was in good agreement. From the simulation it was found that a pressure of 5.7 MPa can be developed if detonation occurred in the end pipe. The simulation can predict the pressure response both in an open and closed pipe.

For industrial application the material of the vent systems should be low electric conductive, high convection heat transfer coefficient, low roughness, leaked tight and unobstructed. The initial conditions and flow rate of the hydrogen should take into account before implement the vent systems.

The University of South-Eastern Norway takes no responsibility for the results and conclusions in this student report.

Preface

This work has been carried out as a part of master's program in Energy and Environmental Technology at University of South-Eastern Norway with a collaborative support from Equinor, an international energy company focusing on low carbon future.

I would like to express my special gratitude to my supervisor Professor Dag Bjerketvedt and Associate Professor Magne Bratland who gave me the golden opportunity to work on this project. Their patience, advice, and creative suggestions from the very beginning of the experiment till the end brought this work ahead. Professor Dag Bjerketvedt offered constant encouragement, support and introduced me to physical apparatus and theoretical knowledge within this short time. His invaluable support and direction helped me to finalize this work.

I would also like to thank my friend Ishmael Nii Nyarko Solomon who did the same experiments focusing on different parameters. We started the laboratory work together and helped each other throughout the experiment.

Thanks also goes to all the people who were directly or indirectly involved in this project from University of South-Eastern Norway and Equinor. I am extremely grateful to my parents, siblings, and friends for their love, prayers, caring and encouragement.

Porsgrunn, May 2024

Rukon Ahmed Eimon

Contents

Nomenclature

Symbol	Abbreviations
DDT	Deflagration to Detonation
BR	Blockage Ratio
RCM	Random Choice Method
CJ	Chapman Jouguet
DOT	Department of Transportation
ASME	American Society of Mechanical Engineers
1D	One Dimensional
3D	Three Dimensional
ER	Equivalence Ratio
NI	National Instruments
NI-DAQ	National Instruments Data Acquisition
VAFM	Variable Area Flow Meters
USB	Universal Serial Bus
SV	Sensor Voltage
GF	Gauge Factor
EV	Excitation Voltage
DAF	Dynamic Amplification Factor
PDE	Partial Differential Equation
EPSC	European Process Safety Centre
SS	Stainless Steel

Symbol	Definition	Unit
φ	Equivalence ratio	-
p	Pressure	MPa
T	Temperature	K
ρ	Density	kg/m^3
u	Velocity	m/s
M	Mech number	-
q	Heat of reaction	j/mole
c_p	Specific heat at constant pressure	j/kgK
c	Speed of sound	m/s
D	Diameter of pipe	mm
λ	Cell size	mm
D_o	Obstacle opening diameter	mm
D_{pi}	Pipe inner diameter	mm
P_y	Maximum allowable pressure at elastic limit	bar
σ_y	Yield strength	MPa
t	Pipe thickness	mm
ε	Strain	-
f	Frequency	Hz
R	Radius of the pipe	mm
v	Poison's ratio	-
G	Shear modulus	GPa
k	Shear correction factor	-

1 Introduction

Carbon emissions are one of the major reasons of global warming where most of it comes from the combustion of fossil fuels. The most abundant hydrogen energy carrier can be used as an alternative to fossil fuel with zero carbon emissions in its combustion. Hydrogen is a lightweight, low-energy-density gas with a minimum ignition energy and a wide explosion limit, making it highly flammable and capable of forming explosive mixtures with air over a broad range of concentrations [1]. Hydrogen is often stored as compressed or liquified hydrogen to achieve a higher volumetric energy density. Emergency venting systems are designed to release excess pressure in the event of a malfunction or unexpected rise in pressure within the storage system. This helps prevent over-pressurization, which could lead to structural failure and potentially catastrophic consequences. A pressure relief valve or rupture disk in the storage system becomes active when the inside pressure exceeds a predetermined limit.

1.1 Background

Several explosions have happened in hydrogen storage due to the failure of the venting system. In 2007, The hydrogen explosion at a power plant in Muskingum, Ohio was triggered by a series of events involving the piping systems and rupture disks during a routine gaseous hydrogen delivery [2]. In Figure 1.1 the situation after the incident is illustrated. The incident began with the failure of rupture disk. An incorrect rating was set between 3600 and 4000 psi (based on DOT instead of the required ASME) even though the vessel rating was 2450 psi. At an approximate pressure of 1800 psi, the rupture disk failed. After the disk failure the released hydrogen was supposed to escape through the vent system and dissipate into the environment above the awning. However, the vent pipe didn't withstand the load of released pressure and one elbow in the vent pipe blew out (see Figure 1.1(b)).

(a)   (b)

Figure 1.1: (a) Explosion occurred while the tube trailer (white tanks) filled the storage cylinder (yellow tanks), (b) An elbow in the vent pipe blew out [2].

As per the investigation by WHA international, an incorrect disk type was replaced during the maintenance and the uncapped vent pipe allowed water to enter and caused corrosion on the pipe and rupture disks. Most importantly, the pipe was constructed out of thin-walled copper which was not rated for the pressure or thrust. The released hydrogen then accumulated under the weather awning and from one of the potential ignition sources, the explosion began which resulted in the death of the truck driver and injured 10 others.

A case history was presented by Bjerketvedt et al. which is demonstrated in Figure 1.2 [3]. In a particular position, the pipe expanded in the radial direction. In that place, the transition to detonation occurred which created a higher internal pressure. The internal pressure rise crossed the maximum allowable pressure and as a result, the elongation crossed the elastic limit and permanent deformation occurred. Fortunately, the pipe didn't rupture.
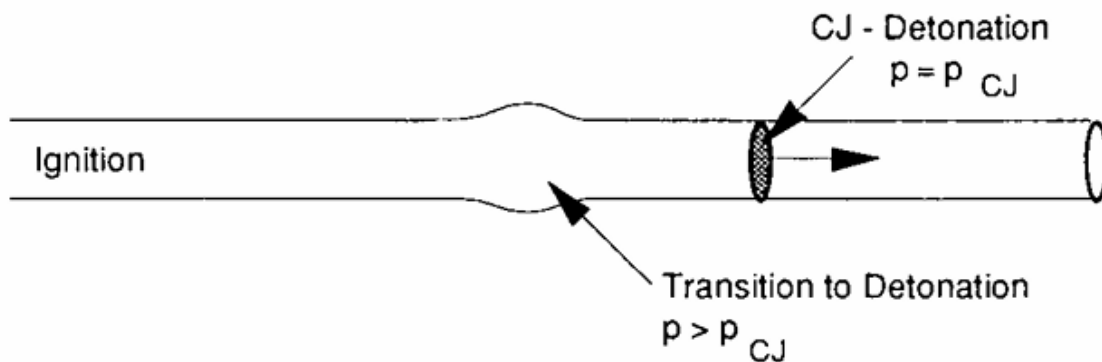

Figure 1.2: A case history of pipe deformation due to transition to detonation [3].

Marchi et al. presented an explosion example in ASME conference. In 2012, a hydrogen fuel cell bus experienced a failure of spring-operated pressure relief valve, releasing about 300 kg of hydrogen which subsequently ignited. Although there were no injuries, the incident raised significant public concern due to an evacuation of three-mile. An investigation led by Sandia National Laboratories identified hydrogen embrittlement of the pressure relief valve material nozzle as a key contributor to the failure leading to the split nozzle and resultant hydrogen release [4].

An incident was presented by EPSC [5] due to the failure of hydrogen emergency vent systems which is shown in Figure 1.3. Pressure safety valve relief the hydrogen in downward movement which ignited and caused explosion. The vent line and relief valve were not checked or repaired after the former release. The possible ignition was because of electrical effects or charged dust particles. It can be concluded that the internal explosion in the pipe is an important phenomenon for safety concerns.
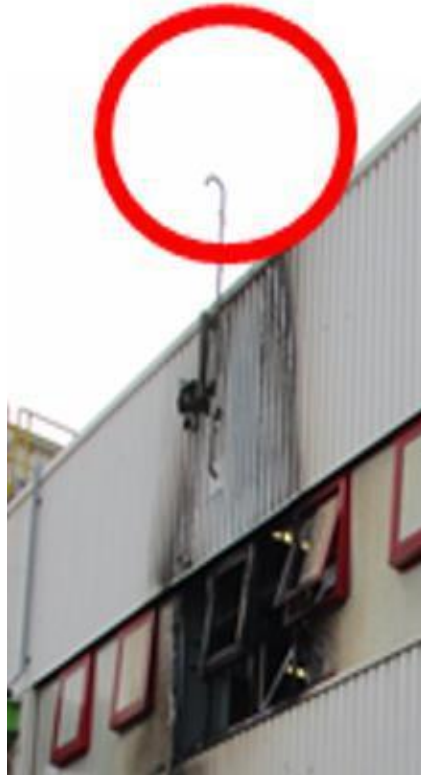
Figure 1.3: Failure of hydrogen emergency vent system and damage [5].

1.2 Hydrogen Emergency Vent Systems

Hydrogen emergency vent systems are a crucial part of hydrogen storage and transport facilities to ensure safety by releasing hydrogen gas. High flammability and low ignition energy are a potential risk factor and care should be considered for designing the vent systems [6]. There are two types of vent systems known as active and passive.

Active vent systems require fans or pumps which can control the flow of hydrogen discharge. It includes sensors and automated controls which trigger the venting system when pressure is exceeding a predefined threshold. These types of vent systems are used where precise control over gas discharge is necessary.

Passive vent systems don't require any power operated components rather mostly rely on natural phenomena such as pressure differences. It is basically designed based on the physical properties of hydrogen and operating conditions of the systems. Passive vent systems are less costly, simple design and easy to maintain compared to active vent. The effectiveness of passive vent systems mostly depends on design, material choice, type of valves or rupture disk, vent stack and so on.

Pressure Relief Valves

Pressure relief valves are designed to release hydrogen gas when the internal pressure is excess of a predetermine level. It doesn't require any external electrical or mechanical power to start its operation. When the pressure rises above the predetermine level the valve automatically opens and after falling the pressure it closes automatically. They are several types such as direct acting, variable back pressure, and pilot operated [6].

Rupture Disks

Rupture disks are sealed membranes which can burst at a specific pressure allowing the gas to be released. Once the ruptured disks break down it doesn't get back to its original shape after the gas release. The disk needs to be replaced once it is activated. The most disadvantage of using rupture disk is that the release will be large and gas release will continue until the pressure difference between outside and inside of the storage is zero.

Vent Stacks or Ducts

Vent stacks are the pathways which ensure safe release of hydrogen from the pressure relief valve to atmosphere. It should be unobstructed, protective from moisture and ice accumulation, leak tight, sufficient pressure rating to withstand the backpressure. The piping immediately upstream of the release should be design with non-sparking metallic material to avoid autoignition [6]. Most importantly, the stack should be designed in such a way to avoid pipe joint, elbow, tee, and other piping components which can act as a resistance to the smoothen flow. The vent stack should withstand deflagration load due to delayed ignition of the gas mixtures, thermal radiation, and DDT inside the stack.

1.3 Objectives

To find out the possible response in emergency hydrogen relief systems review of literature, simulation and experimental study was considered in this study. The experiment is mostly relevant to the Vegeir [7] experiment. The task description is attached in Appendix A and objectives are listed below.

- Review of literature on transition to detonations and propagation of detonations in pipes and the associated loads.
- To simulate the structural loads in pipes subjected to DDT and detonations by using Random Choice Method.
- Perform experimental study of DDT in pipes containing hydrogen and air. Collect relevant data using strain gauges and pressure transducers mostly focusing on pressure.

1.4 Organization of the Report

Chapter 1 represents a brief introduction, example of different explosion incidents due to failure of hydrogen emergency vent system and pipelines, a brief description of hydrogen emergency vent system and objectives. The theory behind DDT development, structural dynamics, an overview on DDT in pipes and relevant literature is presented in chapter 2. Chapter 3 describes the experimental apparatus and setup; experiments result and discussions. Numerical simulations, results and comparison with experimental results are presented in chapter 4. A brief discussion in possible uncertainty in experiments, summary of findings, suggestions to implement a hydrogen emergency vent system and recommendations for future work is illustrated in chapter 5. Conclusion is given in chapter 6. References and Appendix are also included at the end of the report.

2 Theory and Literature Review

This chapter describes the theory behind DDT development in pipe during an explosion and presents the review on transition from deflagration to detonation, propagation of detonation, and the associated load. The review mostly focuses on DDT, pressure, and other closely relevant parameters. In section 2.1 the theory behind DDT development is described and a short description in structural dynamics is given in section 2.2. In section 2.3 an overview is given to DDT develops in pipes and their associated loads.

Why Consider Internal Explosions in Hydrogen Vents?

Due to hydrogen's high flammability, reactiveness, and low ignition energy an internal explosion combusts the gas rapidly which increases the pressure significantly. The rapid combustion can accelerate the flame creating a high velocity shock wave ahead resulting in a detonation or DDT. The detonation or DDT inside a confined space can create an unstable situation inside with a sudden change in pressure and temperature. The vent system should withstand this internal load. It should be designed in such a way to minimize obstructions which could lead to turbulence flow as well as flame acceleration. The internal explosion, detonation and DDT can increase the internal pressure which can lead to failure of the vent systems and end up with a devastating situation. If a structure can sustain the detonation pressure it can mostly overcome the other possible structural load. This is because internal explosions and their corresponding load should be considered before implementing an emergency vent system.

2.1 DDT in Pipes

Deflagration refers to a slow process where the combustion waves propagate at subsonic speeds, and detonation is a fast process propagating at supersonic speeds. Detonation induces a high pressure which leads to devastating structural damage and loss of life and property. A detonation wave travels at a speed of CJ-velocity or even more. Detonation depends on air-fuel mixtures, initial conditions, geometry, detonation cell size, wave speed and many more. Smaller cell size increases the sensitivity and reactiveness of the gas mixtures which initiate and propagate detonation. When a detonation wave passes a particular position a sudden pressure rise is noticed due to the high velocity wave passing. Due to the supersonic speed no loading or instability happens infront of the wave means the gas mixture infront of the detonation wave is undisturbed. That's why a sudden increase is noticed while detonation passes a particular position. Multiple expansion wave travels behind the detonation wave which shows a gradual decrease in pressure. If the initial temperature is higher, it will accelerate the flame resist flame quenching as well as thermal stress in the pipe will be noticed. The wave causes to stress the pipe. The combination of thermal and mechanical stress may create a significant strain in the pipe.

Deflagrations to detonation transition in pipe includes several stages as listed below.

- Forced ignition of mixture.
- Progressing combustion rate by instabilities and turbulent flow in front of flame.
- Formation of shock wave and moving ahead of flame front.

- Detonation wave formation by self-ignition of shock compressed mixtures between shock wave and flame front.
- Self-sustaining Chapman Jouguet detonation velocity.

Ignition of gas mixtures accelerated flame propagation which creates a high temperature and pressure region behind it. This can generate a shock wave travelling in front of the flame front, increase temperature and pressure by compressing the gas mixtures. Shock waves can also create instabilities and turbulence in the mixtures which increase the combustion rate by mixing the fuels and oxidizer more effectively. Turbulence induced in the pipe if it has obstacles, elbow, joint or any other resistance which resist the smoother flow in it. Interactions between shock waves and the flame front, including diffracting shocks reflecting from walls, collision with obstacles, and shock-flame interactions, create hot spots ahead of the flame. The combination of shock waves and turbulent flow can lead to the formation of a detonation wave, which is a self-sustaining supersonic combustion wave that propagates through the mixture.

2.1.1 Ignition of mixtures

Due to the very low ignition energy and high explosivity hydrogen-air mixtures can ignite from a minimum ignition energy from different sources even from a spark from the metallic collisions. The ignition is often defined in two ways as described below [8].

- **Auto-ignition:** If generated heat is greater than the heat loss in the surroundings in a reaction, the self-heating occurs which leads to auto ignition. If the heat loss and generation are equal there will be a critical temperature which leads to auto-ignition.
- **Piloted ignition:** In piloted an external energy source initiates the combustion of the mixture and sustains once the source is removed. A piloted ignition can be a spark, electrostatic discharge, mechanical collisions, adiabatic compressions, ignition by a hot surface and many more.

2.1.2 Flame Propagation

With minimum ignition energy or from autoignition a slow flame known as deflagration can be produced. This slow flame can accelerate following certain conditions and transition to detonations which is known as deflagration to detonation transition or DDT can occur. Also, the flame can be quenched, and no acceleration can happen. Besides, a detonation wave can be decoupled with a lead shock and transition of detonation get back to deflagrations.

Shchelkin found that flame can accelerate due to increase flame surface area, volumetric burning rate, and turbulence of the unburned gas ahead of the flame. He proposed to insert of a metal spiral within the tube to increase turbulence, known as the "Shchelkin spiral," continues to be employed in modern applications to accelerate the flame [9]. It is well known that any obstacle place in the tube results in turbulence and so does accelerate the flame, however, it has dependency on initial and boundary conditions.

Smooth Pipes

After igniting the gas mixtures in a smooth pipe, a laminar and smooth flame propagates at steady rate. The flame propagates through the mixture and expands the gas mixtures causing

destabilization in the flame front. This increases the surface area of the flame accelerating the combustion of the unburned gas ahead of it. The developed heat and combustion products forced the unburned gases ahead of it causing pressure rise and increase the velocity of flame. Due to this thermal expansion the flame accelerated moderately. As the flame reaches the side wall its speed reduces slightly possibly because of flame quenching and a boundary layer developed with the pipe as shown in Figure 2.1. Wall roughness greatly influences the flame acceleration, the interaction between flame and wall formed a turbulent boundary layer and increase the burning velocity. This led to a tulip shape from in the flame front.
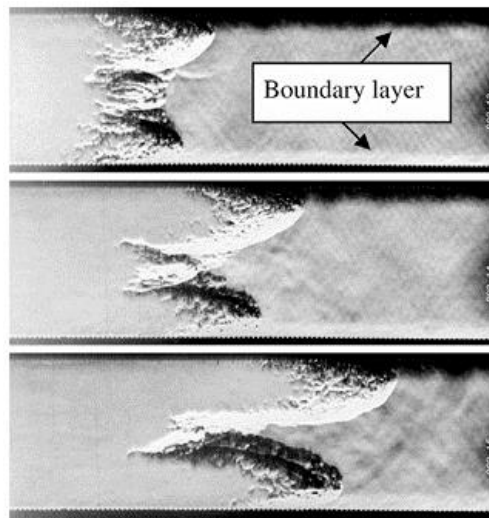

Figure 2.1: Development of boundary layer ahead of the accelerated flame front in a stoichiometric hydrogen-air at 0.6 bar initial pressure [10].

Figure 2.2 (a) presents a stroboscopic image of flame propagation from an experiment conducted by Ellis [11] in a pipe that is 170 mm in length. Initially, the flame expands in a hemispherical shape after ignition at the left end wall. However, as it nears the pipe's side wall, the flame stretches into a finger-like shape. Upon contact with the pipe's side wall, the flame is extinguished, a process that quickly flattens the flame until it inverts, becoming concave towards the unburned gas. This inverted state of the flame is maintained throughout the remaining combustion process. Figure 2.2 (b) shows the inversion flame. Flame inversion refers to a situation where the direction of flame travel reverses relative to the anticipated or initial direction of propagation. This is often observed because of the interactions between the flame front, gas flow, and the boundaries of the pipe. The reflection of shock wave is one of the critical factors in flame acceleration, when it interacts with the flame from it creates a turbulence in the flame and so does accelerate the flame.
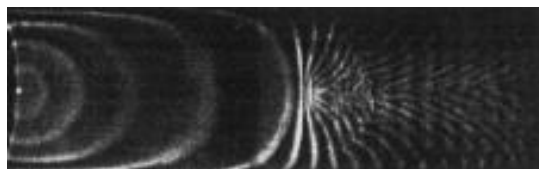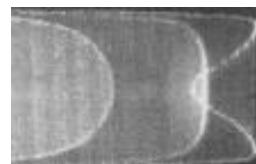
(a)   (b)

Figure 2.2: (a) Flame propagation in a closed pipe , Stroboscopic image [11]., (b) Flame inversion with partly closed pipe [12] .

Obstructed Pipes

Figure 2.3 shows a process of flame acceleration in an obstructed closed channel that begins with a weak igniter at one end which leads to a laminar flame. Due to large-scale turbulence, the flame grows in surface area in a phase known as flame-folding, which increases the volumetric burning rate.
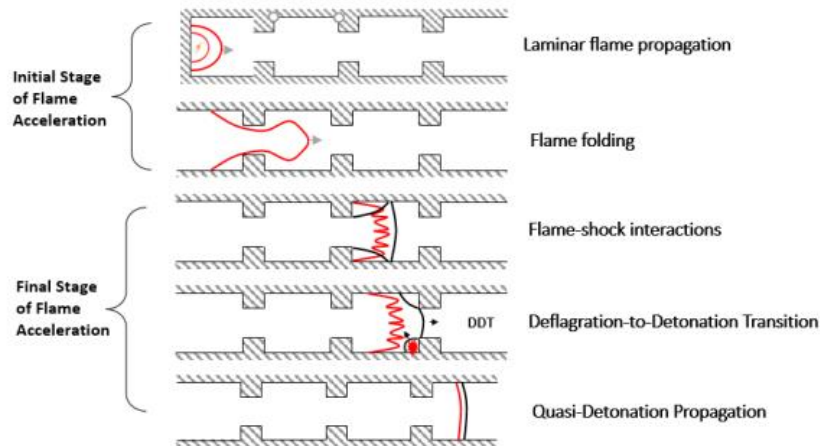

Figure 2.3: Flame acceleration resulting in DDT in obstructed tubes [13].

The increased burning rate results in a higher velocity of the unburned gas ahead of the flame, accelerating the flame. As the flame pushes the unburned gas, compression waves are generated. These waves merge into a leading shock as the flame speed approaches the speed of sound in the reactants, which is around 350 m/s. The interaction between a reflected shock and the flame introduces instabilities, further increasing the volumetric burning rate. When the flame reaches about half the CJ detonation velocity, it transitions into a "fast flame" stage. At this stage, the flame moves supersonically relative to a stationary observer, but it is still considered deflagration due to its subsonic speed relative to the unburned gas ahead. Governed by mass and heat diffusion, this fast flame may transition to detonation under certain conditions, continuing as a quasi-detonation at a velocity below the CJ detonation velocity. This illustrates the potential for a flame to accelerate and transition to detonation in an obstructed channel.

2.1.3 Shock Wave

In gas explosion shock waves occur due to the sudden release of energy which compresses the gas in front of it travelling at a speed faster than sound. Expansion of high-pressure region pushes the surrounding gas, creating a high-pressure wavefront and because of high pressure and supersonic speed it forms a shock wave. Due to the abrupt and rapid changes of flow properties such as pressure, density, temperature, and velocity the shock wave is considered as a discontinuity. The compression is adiabatic but non isentropic. Figure 2.4 shows a shock wave and rarefaction wave travel along with pipe and its corresponding pressure vs distance and different properties across the shock wave. As the gas ahead of the shock is undisturbed the flow velocity ahead of it $v_1 = 0$. The Mach number ahead of shock $M_1 > 1$ and behind of it $M_2 < 1$. Shock velocity and mach number increases as the pressure ratio increases across

the shock. The Rankine-Hugoniot relations describe the relation of states across the shock wave.
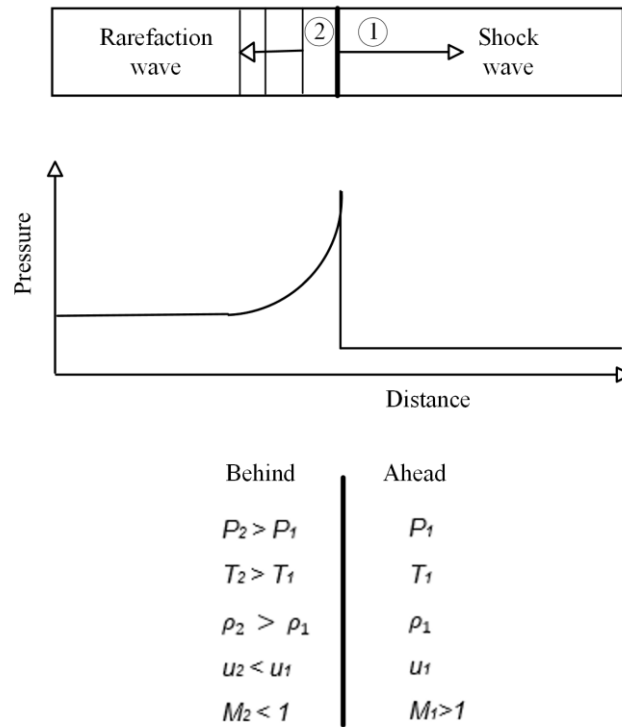
Figure 2.4: Shock wave, rarefaction wave, pressure changes and different properties across shock wave.

Conservation equations

The conservation equations of mass, momentum and energy across a discontinuity are known as Rankine-Hugoniot relations which is given in Equation 2.1, 2.2 and 2.3 respectively. This conservation is considered in a stationary case.

$$\rho_1 u_1 = \rho_2 u_2 \tag{2.1}$$

$$\rho_1 u_1^2 + p_1 = \rho_2 u_2^2 + p_2 \tag{2.2}$$

$$\frac{1}{2} u_1^2 + h_1 + q = \frac{1}{2} u_2^2 + h_2 \tag{2.3}$$

Where $h = c_p T$, c_p is the specific heat at constant pressure, q is the heat of reaction.

Detonation and Deflagrations

Now, if we plot the Rayleigh line and Hugoniot curve together in a $p - \frac{1}{\rho}$ diagram there is two solutions exist, one when the Rayleigh line crosses the Hugoniot curve and when it tangent with the curve. In Figure 2.5 (a) when Rayleigh line crosses the Hugoniot curve (marked as Strong detonation) which gives a large velocity difference across the wave and thus the wave is known as strong detonation wave. Similarly for weak detonation the difference is not that significant and gives a comparatively lower velocity difference across the waves. Again, when the Rayleigh line is tangent of Hugoniot curve as Figure 2.5 (b) there will be only one solution known as Chapman Jouguet solution which implies that this is the minimum velocity that a detonation wave can sustain. For CJ solution u_2 is equal to speed of sound c_2 and the mach number M_2 is one. If u_1 is too low, there will be no solutions in detonation region.
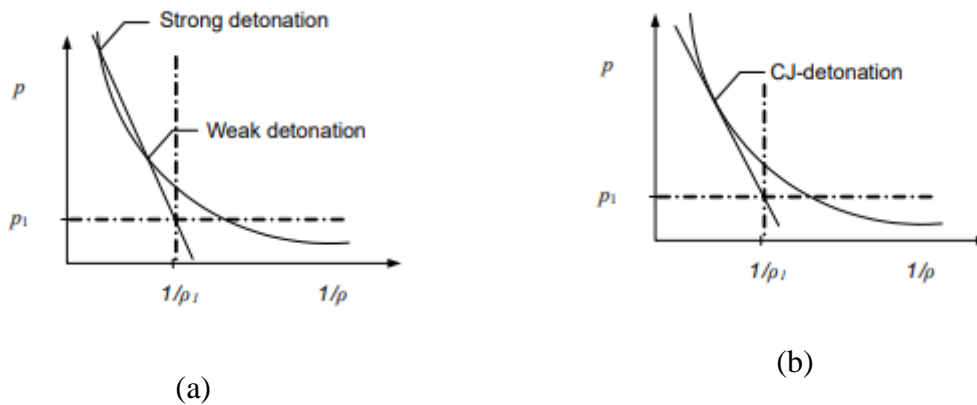

(a)

(b)

Figure 2.5: (a) Strong and weak detonations, (b) CJ-detonations [14].

2.1.4 Cell Width and Critical Run-up Distance

The actual scenario of the wave pattern in a combustion is three dimensional. As the wave propagates towards the axial direction it also shows oscillation towards the radial direction. The characteristic length of this oscillatory wave is known as cell size. The more reactive the mixture the smaller the cell size. Hydrogen concentration, initial temperature and pressure have a great influence on the cell size. The data of cell size at different ER at an initial temperature of 293 K and atmospheric pressure is available in [15] presented in Figure 2.6. At stoichiometric the cell size is minimum, and the size is around 16 mm. For leaner mixtures the cell size is much higher compared with the rich mixture. The reactivity in leaner mixtures is less and the possibility of detonation or DDT is also limited. If the initial temperature and pressure increases, it will reduce the cell size since both increase the reactivity of the mixtures.
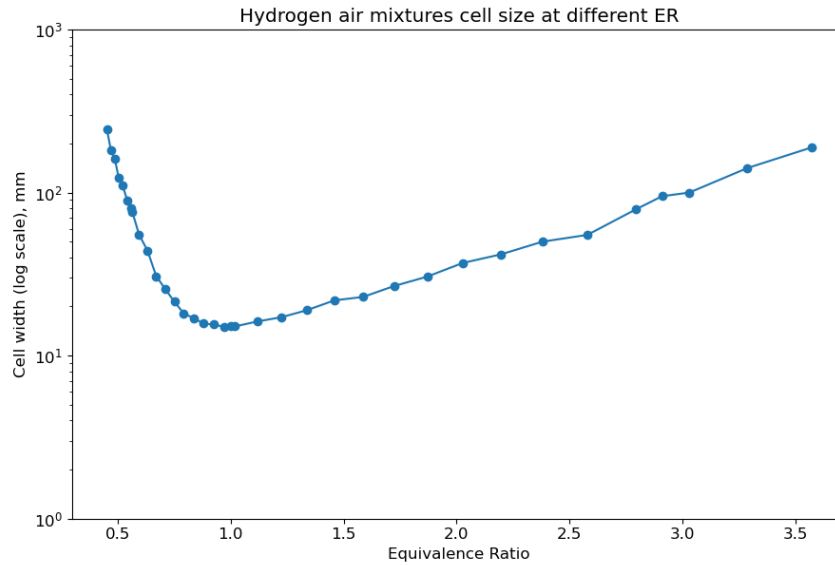
Figure 2.6: Cell width of hydrogen-air mixtures at different equivalence ratio [15].

The exact DDT transition point depends on many factors. The distance from the ignition point to the DDT transition point is known as run-up distance. Mixture composition, initial conditions, pipe roughness, obstacles greatly influence the run-up distance. For the same initial conditions stoichiometric mixture has minimum run-up distance. Obstacles, pipe roughness induce turbulence which accelerates the flame and early DDT occurs. Rise in initial temperature and pressure also reduce the run up distance.

2.1.5 CJ-Velocity and CJ-Pressure

There are three main criteria for the DDT, including CJ-pressure criterion, CJ-velocity criterion and energy sudden criterion [4] [5]. CJ-pressure is the minimum pressure that will be developed if a detonation or DDT occurs. If the pressure in a certain position is greater than CJ-pressure it can be said there might be a DDT transition but not guaranteed since DDT depends on multiple factors. The CJ-velocity is the minimum theoretical velocity that the detonation wave travels through an explosive mixture can sustain. Below this velocity the combustion process is known as deflagration. Energy sudden criteria depend on localized hot spots. Turbulence from obstruction, friction from wall, sudden rise in temperature and pressure, confinement of gas mixtures can create a hotspot and so does initiate a DDT. Here, in this study CJ-velocity, and CJ-pressure are considered for the DDT phenomena. There are several ways to find out the CJ-velocity and CJ-Pressure for different ER in gas mixtures. Here, in this study Shock and Detonation Toolbox – 2021 open source software library which uses Cantera software package to get the CJ-velocity and CJ-Pressure [18]. The initial pressure is atmospheric pressure, and the initial temperature is 300 K. The CJ-velocity for hydrogen-air mixtures at different ER is shown in Figure 2.7.
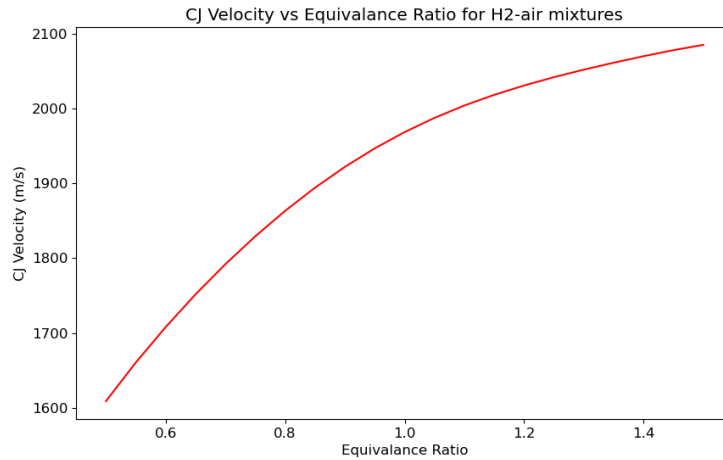
Figure 2.7: CJ velocity of hydrogen-air mixtures at different ER [18].

The CJ-pressure for hydrogen-air mixtures at different ER is shown in Figure 2.8. By using the toolbox, the reflected pressure is found as 5.23 MPa.
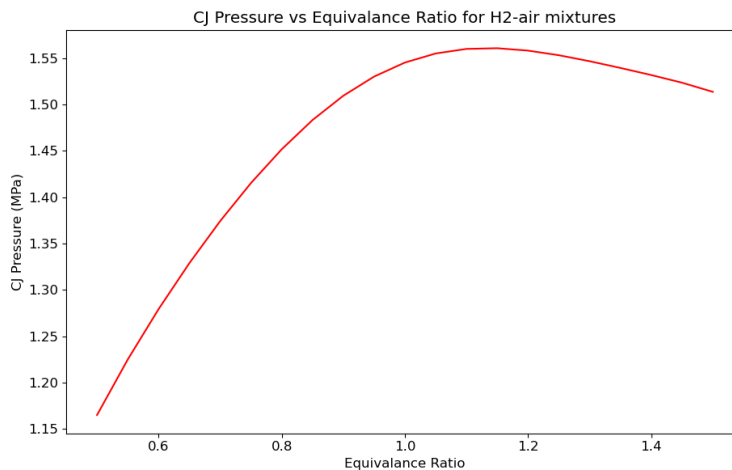
Figure 2.8: CJ Pressure of hydrogen-air mixtures at different ER [18].

2.2 Structural Dynamics

Due to the internal explosion a high velocity shock wave propagates both in axial and radial direction which induces oscillatory force in the pipe. The pipe starts vibrating with a frequency. At first the initial pressure rises to CJ-pressure or even more as wave passing and continuously decreasing due to the expansion wave passing behind the shock wave. If the induced pressure is small enough for the pipe material a sustain oscillation will be developed in the elastic limit of the pipe. However, if the induced pressure surpasses the elastic limit of the pipe, then a permanent deformation as well as structural failure can occur. By considering the radial motion only the natural frequency of the pipe can be calculated using Equation 2.4 [19].

$$f = \frac{1}{2\pi R}\sqrt{\frac{E}{\rho(1 - v^2)}} \tag{2.4}$$

Where f, R, E, ρ and v are natural frequency, radius (53.5 mm), Young modulus (210 GPa) , density (7850 kg/m^3) and poison ratio (0.3) of the pipe respectively. The natural frequency is found as 16.10 kHz.

To predict the structural deflections four critical speeds based on the steady state wave described by Beltmen et al. [20] following the model given by Simkins [21]. The first critical velocity is given in Equation 2.5 which is the lowest critical speed flexural wave oscillations.

$$V_{c0} = \left[\frac{E^2 t^2}{3\rho^2 R^2 (1 - v^2)}\right]^{0.25} \tag{2.5}$$

Where V_{c0} and t are lowest critical speed and thickness (3.6 mm) of the pipe. The lowest critical speed of the pipe is found as 1044 m/s. The second critical velocity can be calculated by using Equation 2.6.

$$V_{c1} = \sqrt{\frac{kG}{\rho}} \tag{2.5}$$

Where V_{c1}, k and G are the second critical speed, shear correction factor (around 1.11 for this pipe) and shear modulus (80.77 GPa calculated from young modulus and poison ratio relations). The velocity is found as 3380 m/s. The wave velocity of a stoichiometric and rich hydrogen air mixtures ranges between the first and second velocity.

For SS 304 tube having thickness and radius 25.4 mm and 152 mm the first critical value was found as 1455 m/s. Dynamic amplification factor was measured for this tube with different wave velocity and the maximum DAF was found in the first critical velocity which is shown in Figure 2.9. The dynamic amplification factor is the ratio between dynamic deflection to static deflection. Since maximum DAF can be induced in first critical velocity and it is one of the most important concerns in dynamic response, only this velocity is considered in this study. The other velocity as well as more details on the dynamic response can be found in [22]. From Figure 2.9 it is found that DAF can be 3.4 due to the first critical velocity. In real cases the DAF can be even higher. Considering, a maximum DAF of 4 can be reasonable in this case.
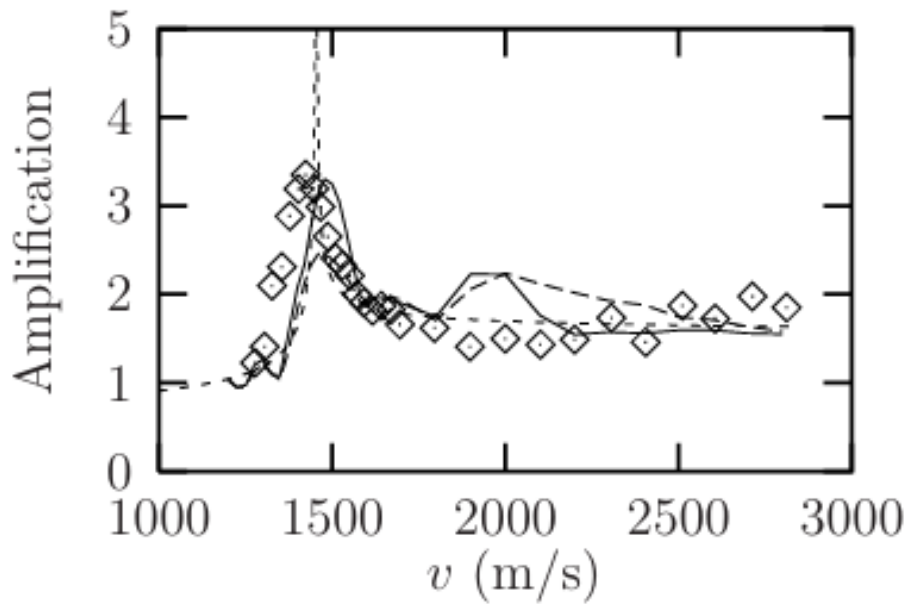
Figure 2.9: Experimental (the square shape) dynamic amplification factor at different wave velocity [20].

2.3 Overview of DDT in pipes and the associated loads

Most of the experimental and numerical study was conducted in homogenous mixture, however, in case of vent system release the hydrogen air mixture is not a homogenous mixture and there is always a concentration gradient in industrial release. Section 2.2.1 describes the previous study on homogenous mixtures and 2.2.2 illustrates a short finding on inhomogeneous mixtures. Table 2.1 represents the summary of some literature along with DDT conditions.

2.3.1 Homogenous mixtures

The phenomenon of deflagration-to-detonation transition (DDT) in pipes depends on several factors such as mixture composition, initial conditions, ignition energy, geometry and physical apparatus [23] [24]. The presence of a bend in the pipe is another hotspot proposed that the transition to detonation is unpredictable and difficult to say when and where the detonation will occur in obstructed pipes [25]. M. Henriksen and his team conducted 20 experiments in a 1 m long obstructed channel where they observed DDT in 10 experiments and it was unexpected to have such results with same initial conditions [26]. The detonation velocity ranges between 1500 m/s and 2000 m/s [24] and peak pressure 15-20 bar [24] [25] for air-fuel mixture combustion. DDT is an unstable phenomenon that maximizes the steady detonation pressure by a factor of 1.5 to 4.5 times [27]. The possibility of DDT is high in case of slightly lean mixture to rich mixture. Vegeir stated that for a DDT within hydrogen-air mixtures, the equivalence ratio φ ranges from 0.79 to 1.95 (optimal 1.2) [23] while Vollmer experiments revealed that DDT more likely develop at an ER greater than 0.68 [25]. Andre's experiment suggest that a minimum φ of 0.88 is required for a DDT [28]. For a stoichiometric fuel-air ratio the pressure ranges from 15-20 bar which is roughly double of maximum pressure produced by a deflagration in the same mixtures [25] [24]. In case of

energy requirements for ignition, 0.02 mj energy can lead to deflagration and 5 kj energy is required for direct detonation [27].

Smooth pipe

Kuznetsov and Dorofeev et al. stated that the diameter of the pipe should be greater than detonation cell size ($D \gg \lambda$) for a DDT. Pipe roughness, turbulent boundary and initial conditions of the mixture influence flame acceleration [29] . In their experiment flame reached a speed of 800 m/s before the onset of detonation. DDT can occur if the pipe is long enough to accelerate the flame and the geometry allows it to sustain the detonation [3]. Maeda et al. experimental results showed that flame accelerated up to 400 m/s in a smooth pipe without any DDT but DDT occurred with a rough wall surface for the same conditions [30]. The run-up distance decreases as the initial pressure and temperature increases [29]. A decrease in hydrogen volume concentration from 30 to 12 % increase the run up distance by a factor of 5 or even more [31].

Obstructed Pipe

Studies have shown that DDT can be significantly affected by blockage, elbows, tees, bends, pipe joint or any other resistance which increases turbulence and flame velocity [23] [22] [27] [25] [32]. The obstacle accelerates the flame propagation and influences the overpressure of the system. Vegeir suggest that a BR ranges from 0.572 to 0.965 is more effective for DDT phenomena with an optimum BR of 0.921 [23]. In case of multiple blockages, the BR and spacing of blockage is an important parameter to develop DDT. Vollmer et al. experimental study found that with a BR 0.3 and spacing 100 mm DDT was observed, however, for the same BR having a spacing of 300 mm no DDT was observed because of inefficient mixing keeping a large portion unmixed. On the other hand, with a BR 0.6 and spacing 100 mm DDT was never observed because the detonation shock wave cannot develop due to narrow spacing and large blockage [33]. Pipe bend is a hotspot for DDT due to internal explosion [25]. Robert and his team conducted experiments in straight pipe, 90^0 bends, and 0.2 BR baffle and found the run-up distance 12.1 m, 11.8 m, and 10.9 m respectively [32]. The flame speed is shown in Figure 2.10. The flame speed immediately rises to 800 m/s and 550 m/s from 200 m/s due to the present of baffle and bend respectively. The findings revealed the significance of pipe bends in flame acceleration and DDT.
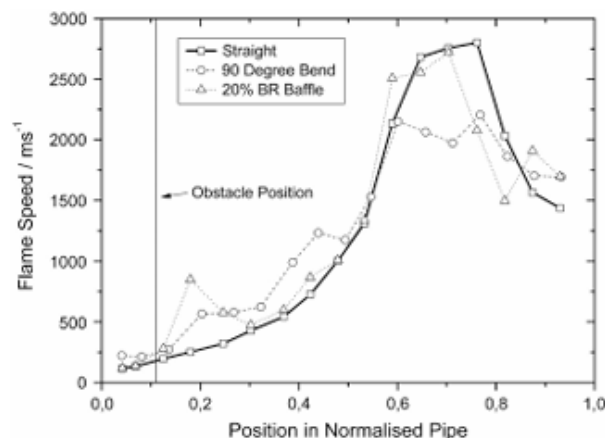

Figure 2.10: Flame speed for hydrogen-air explosions in pipe [32].

Pipe length is also an important geometric parameter in DDT phenomena as the flame propagation can be affected by reflection waves from the opposite end of a closed pipe[23]. The pressure from a DDT increases if DDT occurs close to a dead end due to unburnt gas "piling up" ahead of the supersonic flame front [27]. Zhonglin et al. experiments showed that DDT didn't occur with a 4m pipe length for the BR 0.3 to 0.75. For 6m length pipe DDT occurred after 4m for higher BR and for 8m long pipe DDT occurred between 2 to 5 m length for all BR [34]. For a closed pipe high flame speed is required to generate DDT, flame accelerates at the beginning but start decreasing towards the end of pipe as the pipe end obstructs the flow [24]. From the closed end the detonation reflected as a shock wave which induced a flexural wave and interfered with the incident wave. The peak dynamic load factor and the peak pressure were increased by 50% due to reflection from the closed-end pipe. DDT can induce pressure excess of CJ pressure or reflected CJ pressure [22]. White observed the reflected pressure of stoichiometric hydrogen-air explosion was 170 atm which is 4.5 times higher than CJ reflected pressure [35]. Higher pressure only obtained when the detonation occur at the close end of the pipe and the peak pressure can be 500 bar twice the computed value for a reflected CJ detonation [22].

Du et al. experimental results are shown in Figure 2.11 which represents the hoop strain response induced by detonation wave. A sustain oscillation was noticed possibly because of flexural wave passes after the detonation passed the strain gauge [36].
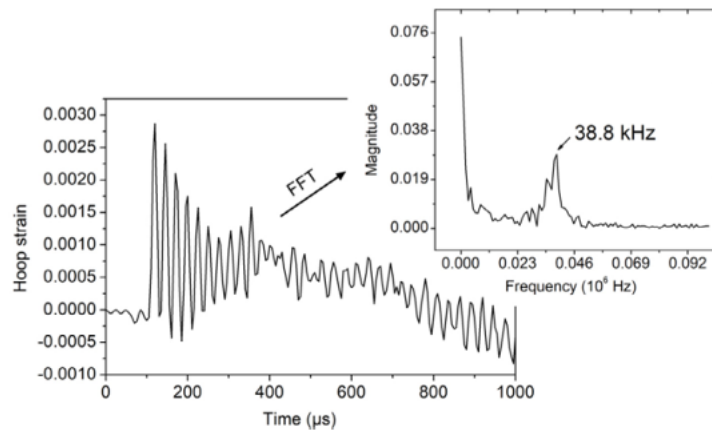
Figure 2.11: Hoop strain response due to detonation wave propagation [36].

RCMLAB simulation was performed by Vegeir to simulate the burning velocity, flame speed, and overpressure and compared with the experimental results. An illustration of simulated and experimented pressure at the ignition points of a 4 m pipe having 30 % hydrogen volume ratio and 0.921 BR is shown in Figure 2.12 [23]. The simulation result showed that it can predict the real explosion scenario quite well.
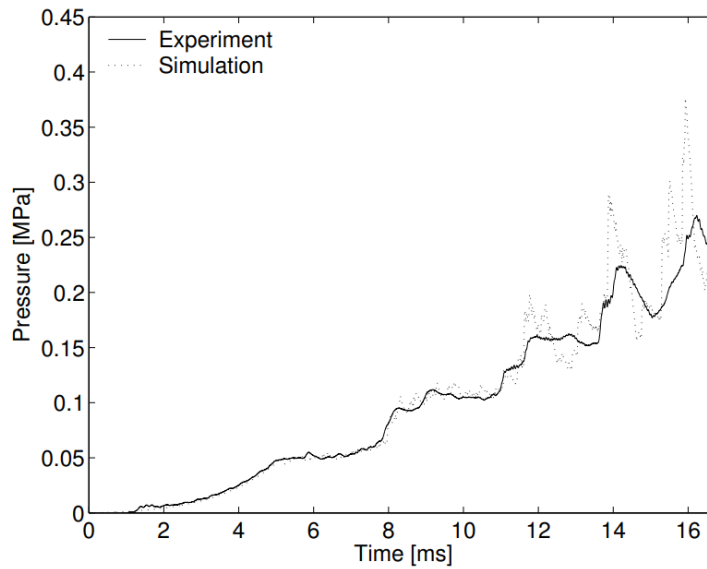
Figure 2.12: Simulated and experimented with overpressure at the ignition point of 4 m pipe for 30 % hydrogen volume with 0.921 BR [23].

Du et al. simulated pressure histories demonstrated that the pressure initially spiked to a close value of CJ pressure of 6.1 MPa which was align with the result from experimental value (see Figure 2.13).
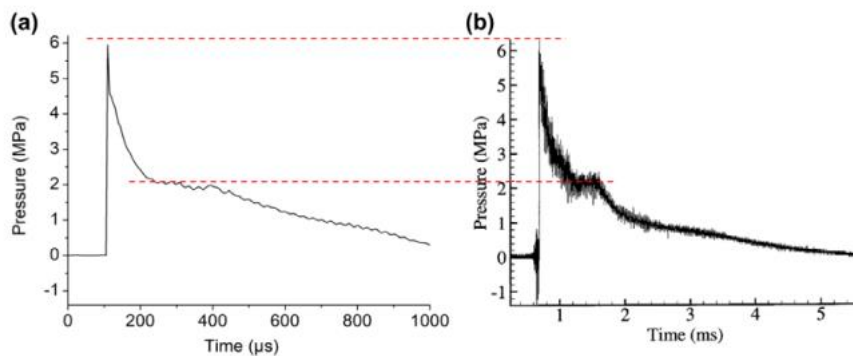
Figure 2.13: a) Simulated pressure result in the pre-flawed pipe [37], b) Experimental result recorded in the detonation pipe [36].

2.3.2 Inhomogeneous mixtures

Inhomogeneous mixtures of hydrogen and air can be developed during venting, especially when there is any leak, and the hydrogen can be stored at the top of a confined space. Andre's experimental study on inhomogeneous hydrogen-air mixtures revealed that DDT showed a similar event as homogenous mixtures [28]. Vollmer et al. experimental investigation revealed that that the maximum flame velocity was 8% lower in inhomogeneous mixture compare to homogenous mixtures [33]. DDT was observed with a concentration of 28 % hydrogen. Detonation failing was observed in one experiment but a subsequent second onset of detonation was developed. It implies that detonation can propagate despite being inhomogeneity. Boeck's investigation suggest that concentration gradient of inhomogeneous

mixtures greatly influence DDT [38]. The inhomogeneous mixture shows higher peak pressure and early DDT with a steep concentration gradient. For design purposes considering homogenous mixture may lead to underestimate the potential risks.

Table 2.1 presents the overview of DDT occurrence in different literature with different properties.

Table 2.1: Type of fuel, Blockage Ratio, DDT, and Equivalence Ratio in different literature.

Fuel	Type of Blockage	Blockage Ratio	DDT	Position of DDT	Equivalence Ratio	Reference
Hydrogen	No	-	Yes	At 5m distance	1.0	[29]
Hydrogen	No	-	Depend on pipe roughness	At 120 mm distance	1.0	[30]
Hydrogen, propane, methane	Single Circular obstacle	0.57 - 0.97	Depend on BR and ER	After obstacle, in the end pipe	0.79 - 1.95	[23]
Hydrogen	-	-	yes	-	1.0	[27]
Hydrogen	Multiple cylinder	0.77	50% with same conditions	After the obstacle	1.2	[26]
Hydrogen, methane, propane	90^0 bends, baffle	0.1 - 0.3	yes	After the obstacle	1.0	[32]
Hydrogen	Multiple circular	0.3 – 0.6	Depend on BR and ER	After the obstacle	0.6 to 0.9	[33]

3 Experiments

Several experiments with different H2-air Equivalence Ratio were conducted to observe the DDT, associated load, and structural response of the pipe. In this chapter, the complete experimental setup, experiment procedure and results are described. Apart from strain gauge the experimental setup is mostly relevant with Vegeir experiment [7].

3.1 Experimental Setup

A complete setup of the experiment is shown in Figure 3.1. Four pressure transducers, amplifiers, and PicoScope 4000 series were used to measure the internal overpressure of pipe. Three rosette strain gauges, NI-9237, NI-9234, NI-9944 were also used to measure the strain of pipe due to internal load. Trigger unit to deliver trigger signal to PicoScope, NI-9234 and spark ignition which was the ignition source in this experiment. H2 and air were supplied from compressed cylinder and air compressor, and their flow were controlled with VAFM. These units are described in the following section in detail.
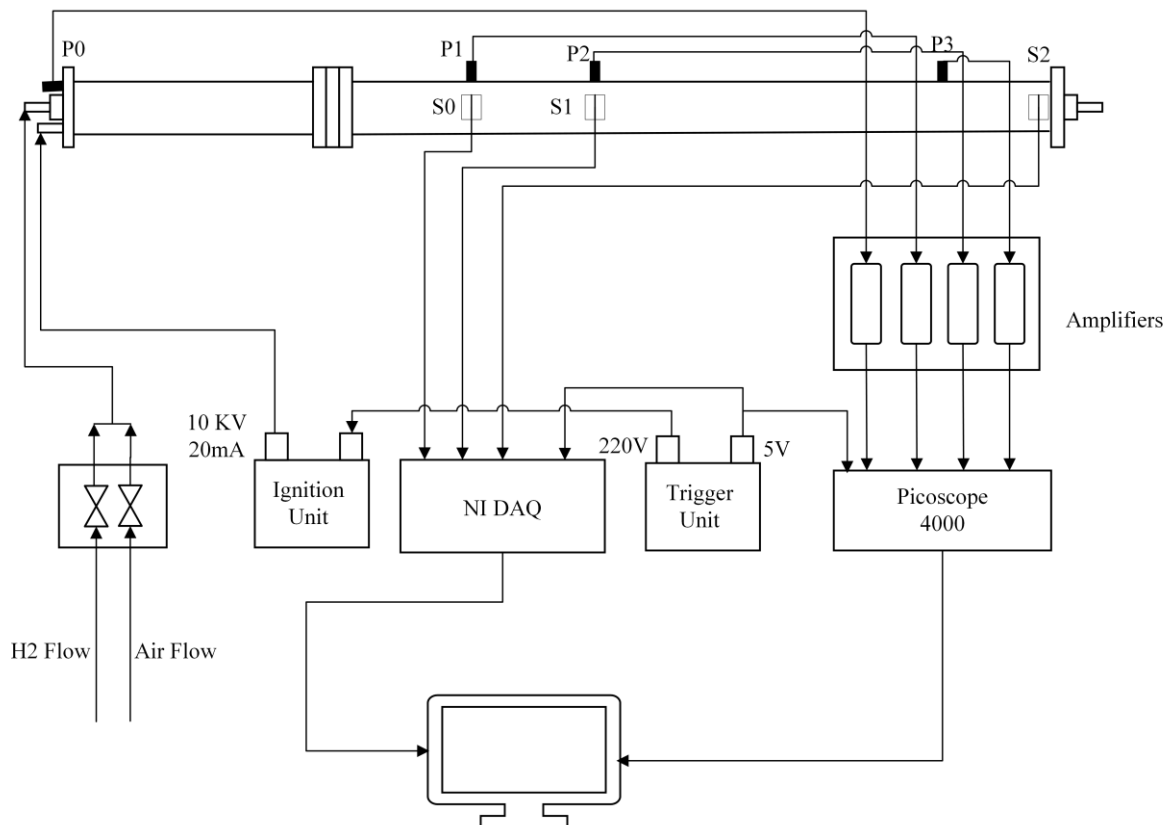

Figure 3.1: Visual representation of experimental setup.

3.1.1 Pipe

Two carbon steel (C22.8) pipes of 1 m and 3 m length having inner diameter and thickness of 107 mm and 3.6 mm respectively have been used in these experiments.

A visual representation of the pipe is given in Figure 3.2. Flanges were also available in both ends of the pipe to connect with blockage, pipe, or valve. An obstacle of opening diameter 30 mm was placed between the junction of the two pipes which accelerated the turbulence of the flame propagation. The BR ratio for this obstacle was 0.921 which is calculated by Equation (3.1).
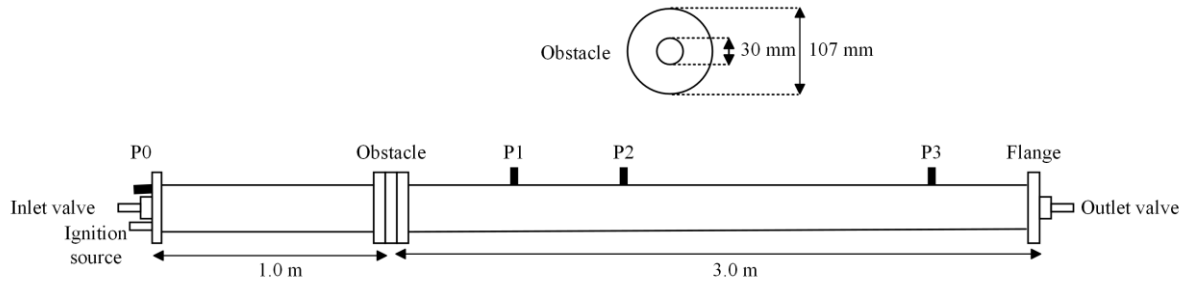

Figure 3.2: A schematic diagram of pipes with obstacle, valve, ignition, pressure transducers and strain.

$$BR = 1 - (\frac{D_o}{D_{pi}})^2 \tag{3.1}$$

Where D_o and D_{pi} are obstacle opening diameter and pipe inner diameter respectively. Rubber rings were placed between the junction for leakage barrier. At the other end of the 1 m pipe, a manual control valve for the inlet of hydrogen and air mixtures, a center mounting point for the ignition source, and the pressure transducers P0 were attached. The three other pressure transducers P1, P2, and P3 were placed 0.5 m, 1 m, and 2.5 m apart from the junction of the two pipes respectively. At the other end of the 4 m pipe, another manual valve was attached to release the gas through ventilation.

The maximum allowable pressure within the elastic limit for a material can be calculated by Equation (3.2).

$$P_y = \frac{2\sigma_y t}{D_{po}} \tag{3.2}$$

Where P_y, σ_y, t, and D_{po} maximum allowable pressure in the elastic limit, minimum yield strength, pipe thickness and outer diameter of pipe accordingly. The minimum yield strength of C22.8 material is 250 MPa and from Equation (3.2) the allowable pressure is found as 157 bar.

3.1.2 Pressure Transducers and Amplifiers

Kistler 7001 and Kistler 603B pressure transducers were used to measure the internal pressure of the pipes which have a stainless-steel sensor body. The Kistler 7001 has a maximum pressure range of 250 bar, natural frequency 570 kHz and sensor diameter 9.5 mm while the Kistler 603B has 200 bar maximum pressure range, 400 kHz natural frequency and 5.5 mm sensor diameter. Kistler 7261 pressure transducers were used to measure the static pressure which has a maximum pressure range from 10 bar. It has a short rise time, high frequency, and sensitivity. The measured pressure is acting on a piezo electric quartz crystal

that transforms the pressure into electrical voltage [V]. The pressure transducers have a unique sensitivity [V/bar]. Silicone gel was placed on the top of transducers to prevent it from over temperature. Mounting adapters were used to place the transducers inside the pipe which is shown in Figure 3.3. More details on Kistler pressure transducers can be found on their official website [39].

Pressure transducers were connected to individual amplifiers. These are Kistler 5011 and Kistler 5041. Every transducer has its own sensitivity setting and it was set before operation. The mechanical sensitivity can be set based on how much pressures bar should be shown against 1 V signal. All the amplifiers were set 20 bar/V.
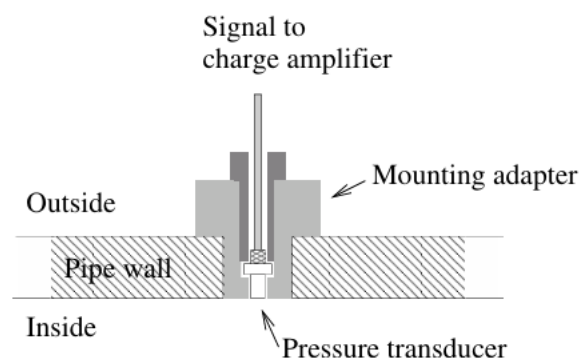
Figure 3.3: Pressure transducers mounting inside the pipe [23].

3.1.3 Strain Gauges

When a material is subjected to a force it's either elongated or compressed due to the force, a strain gauge is a device which measures this deformation known as strain of material. A single strain gauge can measure the strain in only one direction and a rosette strain gauge can measure the strain in multiple directions, usually in three directions. The basic working principle of strain gauge depends on Wheatstone bridge mechanism. The elongation or contraction of strain cause to change the resistance and as a result to change the voltage. In this study, 120-ohm rosette strain gauge was used which was connected to 120-ohm NI-9944. The three-quarter bridge strain gauge was placed at $0°, 45°$ and $90°$ angle in the rosette strain gauge. Both are two resistant of Wheatstone bridge. The output of NI-9944 was connected to NI-9237. The remaining two other 120-ohm resistance were provided by NI-9237. All four resistances should be the same. NI-9237 related to NI-DAQ and finally to the computer. Calibration was done before every experiment. A factor is needed to convert the voltage signal to strain which is described in section 3.2.9. More details on strain gauge working principle can be found on [40] and also on NI's official website [41].

3.1.4 Signal Triggering

A trigger system was used to provide signal to ignition system, PicoScope 4000, and NI-DAQ. A picture of the trigger system is shown in Figure 3.4 (a). The trigger system had an input voltage of 220V, inside of it there were electronics and transformers which produce

220V and 5V output signal. The 220V output signal goes to the ignition unit and 5V signal was connected to both NI-DAQ and PicoScope 4000. A manual switch was placed at the top of the trigger systems which accelerates the whole systems. In both NI-DAQ and PicoScope 4000 the 5V signal was set as the reference for data acquisition.

(a)   (b)
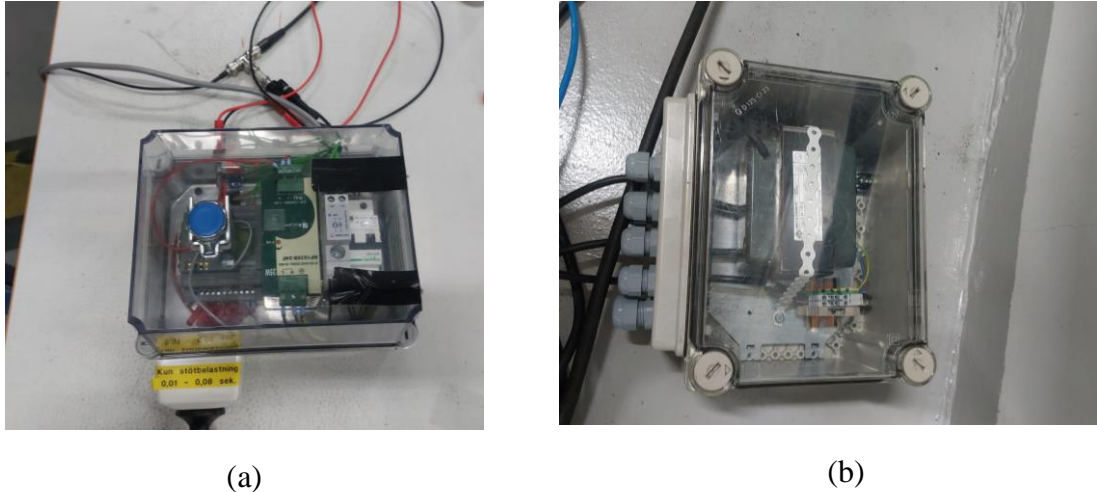
Figure 3.4: (a) Signal triggering system, (b) Ignition unit.

3.1.5 Ignition System

A spark ignition was used to ignite the mixtures which is shown in Figure 3.4 (b). There is a transformer inside the ignition system which converts the 220V input voltage to 10 KV high voltage. The ignition system transfers a current of 20 mA which is regarded as a weak ignition energy. The electrode was placed at an approximate distance of 2 mm from each other. From the first spike response in pressure transducer P0 the ignition time can be determined. This ignition signal has just a few sampling points, preferably less than 5. There is always an ignition delay from the triggering time and ignition occurrence.

3.1.6 Gas Handling Unit

Hydrogen and air gas mixtures were used at atmospheric pressure and homogenous condition. Hydrogen was supplied from industrial grade compressed cylinder and air from gas compressor. Variable Area Flow Meters (VAFM) were present to control the flow and maintain the equivalence ratio. After passing through the VAFM both pipes connected and entered as a single unit in the explosion pipe. An image of the gas handling unit attached in Figure 3.5.

Figure 3.5: Gas handling unit. The left one controls the hydrogen flow and the right one controls air flow.

3.1.7 Data Acquisition and Recording

PicoScope 4000 series was used to record the pressure signal from pressure transducers. A PicoScope is a digital version of oscilloscope which can connect directly to the computer with USB, and it takes power directly from the computer, so, no external power source is required. It is a high-performance test instrument which measures and displays the voltage signals. This device has an 8-input port which can directly connect to the amplifiers. Also, the signal triggering was connected to one of the ports. Pico 7 software was installed to connect the scope. Pico 7 has several features where the voltage range, sampling rate, triggering conditions, pre triggering and time length can be defined as per the requirements. In these experiments the voltage range was set to -5V to +5V since the mechanical factor in the amplifier was set to 20 bar/V. Data was collected at a sampling rate of 40 MHz over a period of 100 ms with 10% pre-triggering which measured the signal over 90 ms from the triggering till the end. Finally, the pressure data was saved as a csv file for further processing.

NI FlexLogger software was used to set up strain gauge and for strain data acquisition. Data was collected at a sampling rate of 30 kHz for 1s and saved as an excel file for further processing.

3.1.8 Data Post Processing

To handle and analyze the data Python programming language was used. With the programming both the pressure and strain data were plotted, different calculations like detonation velocity, reflected shock wave velocity, sampling rate was also done. Although the pressure amplifiers and strain gauge calibrated before every explosion, the data recording still showed some initial value possibly because of the high-pressure mixture flow. Signal noise was noticed in the data recording. To minimize the noise and smoothen the data Savitzky-Golay filter width a filter window 9 and poly-order 1 was used before post processing.

3.2 Results and Discussions

A total of 30 experiments were conducted including test experiments in different ER with a sampling rate of 40 MHz in PicoScope and 30 KHz in NI. The results of these experiments are summarized in Table 3.1. Besides, static pressure test, NI vs PicoScope pressure test was also conducted. The results of these tests are discussed in more detail in the following sub-section.

Table 3.1: Summary of hydrogen-air explosion result at different concentrations.

φ/ Volume %	Test no.	Overpressure [MPa]			Maximum reflected overpressure [MPa]	Wave velocity [m/s]	Reflected wave velocity [m/s]	DDT	Comments
		P1	P2	P3					
0.6 / 20	11	0.28	0.35	-	-	751	-	-	In test 11 no response at P3
	12	0.36	0.32	0.23	P3 = 0.47	692	-	No	
	23	0.44	0.34	0.21	P3 = 0.42	709	-	No	
	30	0.43	0.20	0.23	P3 = 0.40	711	-	No	
0.8 / 25	13	0.88	1.23	0.39	P3 = 2.03	880	1417	End of pipe	In test 25 possible error in air-fuel composition
	14	0.58	1.10	0.29	P3 = 1.41	816	1140	End of pipe	
	24	0.68	0.75	0.44	P3 = 2.56	917	1350	End of pipe	
	25	1.07	1.40	1.27	P3 = 1.35	1887	1174	Between P1 and P2	
1.0 / 30	15	-	1.36	1.44	P3 = 1.45	1980	1236	-	In test 15 very low response at P1
	16	1.0	1.45	1.36	P3 = 1.43	1978	1247	Between P1 and P2	
	26	0.88	1.79	1.20	P3 = 1.77	1961	1246	Between P1 and P2	
	27	1.09	1.81	1.28	P3 = 1.44	1977	1245	Between P1 and P2	
1.2 / 33.5	17	1.28	1.36	1.43	P3 = 1.31	2062	1207	Possibly between P2 and P3	-
	18	1.85	1.40	1.41	P3 = 1.33	2064	1215	Between obst and P1	
	28	1.20	1.84	1.54	P3 = 1.40	2042	1235	Between P1 and P2	
	29	1.0	1.34	1.27	P3 = 1.44	2039	1278	Possibly between P1 and P2	

3.2.1 Static Pressure Test

To evaluate the response of pressure transducers a static test was conducted. A static pressure transducer was placed at 3.0 m keeping all other pressure transducers in their position. Air is supplied from the inlet valve keeping the outlet valve closed. After an approximate 30s inlet valve was also closed. At time 36s outlet valve was opened. The result of the static pressure test is shown in Figure 3.6 (a). Between 30s to 36s the pressure was decreasing which indicates that there was leakage possibly between the junction of pipes, obstacle, valves, pressure transducers, gas inlet point or in the ignition inlet point. Since the initial pressure throughout the experiment was considered as atmospheric pressure this minor leakage will not create any major difference in the results. But there is a possibility of air entering the pipe and making the mixtures leaner. Although the pressure amplifiers were calibrated before the test it was noticed that P1 and P2 have some initial signal. The same problem was noticed during the experiments. To overcome this, the initial value of pressure transducer was subtracted from the whole record. After the subtraction the starting of all pressure transducers align with 0 position but showed offset as time passes which is shown in Figure 3.6 (b). At the beginning the pressure response was almost identical in all pressure transducers, however, as pressure increases the difference is increasing.
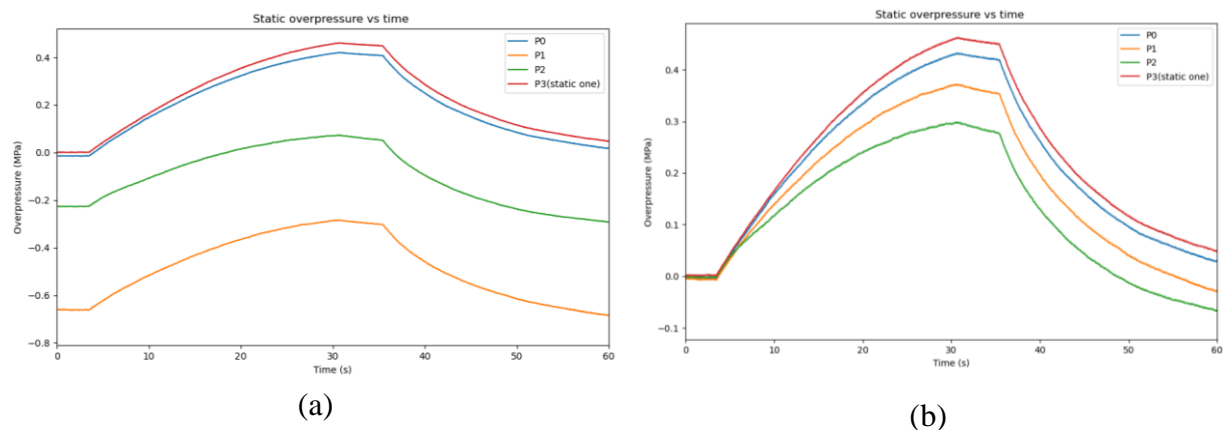

| (a) | (b) |

Figure 3.6: (a) Static overpressure vs time, (b) Static overpressure vs time after aligned all pressure transducers initial pressure to 0 bar.

3.2.2 PicoScope vs NI

To verify the data acquisition and signal noise of PicoScope and NI, pressure response at P3 was measured for an equivalence ratio of 0.8. Both data were recorded at a sampling rate of 30 KHz. Both pressure responses showed quite a similar trend; however, the NI instrument demonstrated a lot of noise throughout the pressure acquisition as shown in Figure 3.7. In the plot NI data is placed 1 MPa higher to visualize the difference. There might be several reasons behind this noise, but the high voltage ignition and the normal electrical wire used to connect the strain gauge was the major reason. High voltage ignition source can create a high electromagnetic interference which affects electronic instruments like strain gauge. Rapid change in current creates an unexpected voltage change in the strain gauge known as noise. Besides, normal electrical wire is not shielded and any electromagnetic interference from the surroundings can create noise.
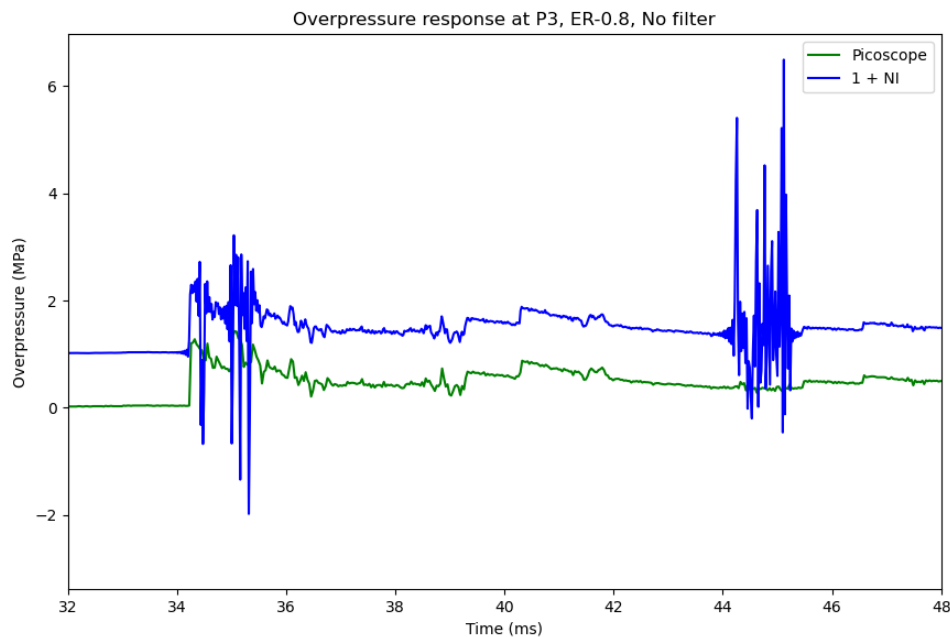
Figure 3.7: Overpressure response in PicoScope and NI at P3, $\varphi = 0.8$ with no signal filtering. NI data is placed 1 MPa higher to visualize the difference.

After applying Savitzky-Golay filter to a filter window size 9 and poly-order 1 the noise is reduced in NI as shown in Figure 3.8. In case of no filtering the NI first peak point is quite align with PicoScope but after filtering it shows some offset with PicoScope reading. The same difference is noticed all the way to the end of the reading. After filtering the noise was reduced in NI but showed some unreliable pressure response at 34 to 35.8 ms and 44 to 45.7 ms which was just noise. The higher window size and higher poly-order can smoothen the data but may make a significant difference from the actual value. All the strain gauge data acquisition was measured with NI and the same noise problem was noticed. It can be concluded that the PicoScope data acquisition has better accuracy compared with the NI.
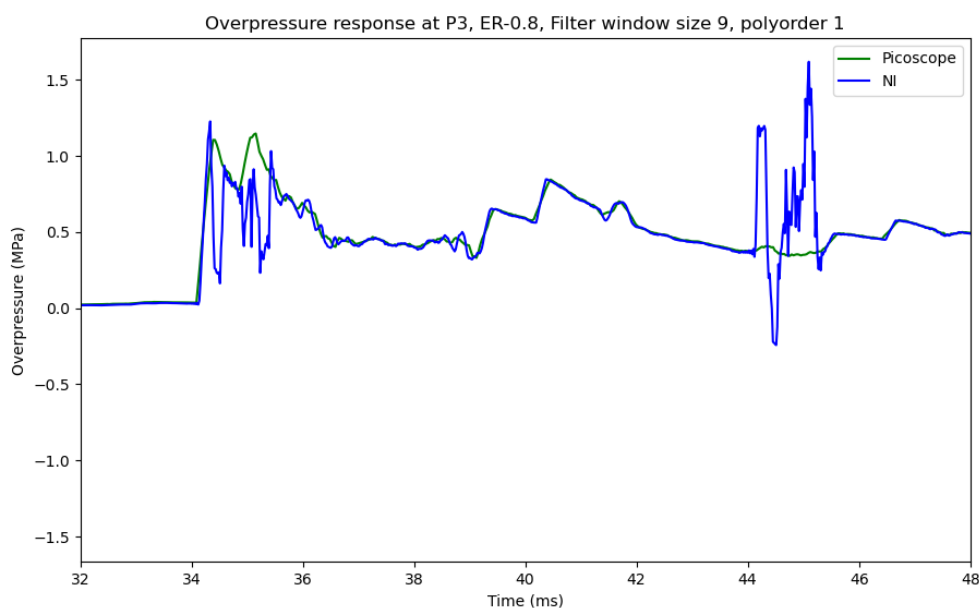

Figure 3.8: Overpressure response in PicoScope and NI at P3, $\varphi = 0.8$ with filter window 9 and poly order 1.

3.2.3 Hydrogen-Air Explosion at $\varphi = 1.0$ (30% Hydrogen)

A total number of 4 experiments were conducted with hydrogen-air at $\varphi = 1.0$. Detonation occurred between P1 and P2 in three experiments and in test no 15 a very low response was found in P1 possibly because of incorrect setting of amplifiers. The result of experiment 16 is shown in Figure 3.9. Ignition had an approximate delay of 20.33 ms from the trigger time. The flow of unburned gas in front of the flame created a turbulent flow on the other side of the obstacle. This turbulent flow accelerates the flame propagation and transition to detonation occurred after the obstacle. The overpressure due to the shock wave travelling ahead of the flame for P1, P2, and P3 were recorded as 1.0 MPa, 1.45 MPa and 1.36 MPa respectively. Detonation occurred between P1 and P2. Based on the shock wave travel time from P1 to P3 the detonation velocity was measured as 1978 m/s. When the shock wave reaches the end wall, it reflects and travels in the opposite direction of incident shock wave and flame propagation. The overpressure due to the reflected shock wave in P0, P1, P2 and P3 were recorded as 0.83 MPa, 0.89 MPa, 0.88 MPa and 1.43 MPa respectively. It is noticed that the reflection pressure in P3 is higher than the incident pressure in P3. When the shock wave reflects, the gas mixtures experienced a compression near the close end of the pipe.

Figure 3.9: Experimental results of overpressure at different positions, shock wave, reflected shock wave, and ignition time at $\varphi = 1.0$ for hydrogen-air mixture explosion in 4m pipe (test no. 16).

The reflection and compression create a confined space which forces the molecule to stay closer, increasing the number of collisions which results in rising pressure. The energy from the incident wave is converted to kinetic energy of the molecules which raises the pressure. When the shock wave passed a particular position, the pressure decreases gradually due to the multiple expansion wave travel behind the shock wave in the opposite direction of shock wave. The reflection wave is coupled with the expansion wave and leads to a higher wave which means higher pressure. When P3 rises again due to the reflection the initial pressure of P3 is approximately half of the incident shock wave pressure. The reflection shock wave is drawn based on the P2 and P0 reflection pressure response and extended all the way to the

end of the pipe. Although the P0, P1, P2 reflection pressure response is quite aligned with the reflection wave, P3 reflection pressure response shows a delay. When the shock wave travels, the gas mixtures behind it follow the shock wave. The reflection wave must overcome this velocity which reduces the actual reflection wave velocity and thus the reflection pressure response delayed at P3. The effect of this gas mixture velocity is mostly in the end of pipe that's why the reflection wave is drawn as dotted line from P3 to P2. The reflection wave velocity was 1247 m/s.

3.2.4 Hydrogen-Air Explosion at $\varphi = 0.8$ (25% Hydrogen)

At $\varphi = 0.8$ detonation occurred in the end of pipe in test no. 13, 14 and 24 but in test no. 25 detonation occurred between P1 and P2. There are two possible explanations for test no. 25. It was noticed that when the air compressor refill by itself the air flow rate fluctuates a little even though the VAFM was fixed. Low air flow means higher φ and the mixture is most likely to be a stoichiometric mixture. Test no. 25 was the 6th test on that day and the interval between tests is approximately 20 to 30 minutes. It was noticed that after a few explosions the pipes became heated, and the initial temperature was no longer room temperature. Since the initial temperature has a great influence on DDT, especially, it resists the flame to be quenched, this may be one of the reasons for early DDT in test no. 25.

The result of experiment 24 is shown in Figure 3.10. The ignition had an approximate delay of 22.21 ms. The overpressure at P1, P2, and P3 were recorded as 0.68 MPa, 0.75 MPa and 0.44 MPa respectively. The deflagration wave velocity was recorded as 917 m/s. No detonation occurred as the wave propagated towards the end of pipe. When the shock wave reached the end wall transition to detonation happened. The reflected overpressure was recorded as 1.04 MPa, 1.0 MPa, 0.86 MPa and 2.56 MPa in P0, P1, P2 and P3 respectively. 2.56 MPa was the maximum reflected overpressure recorded throughout the experiments.
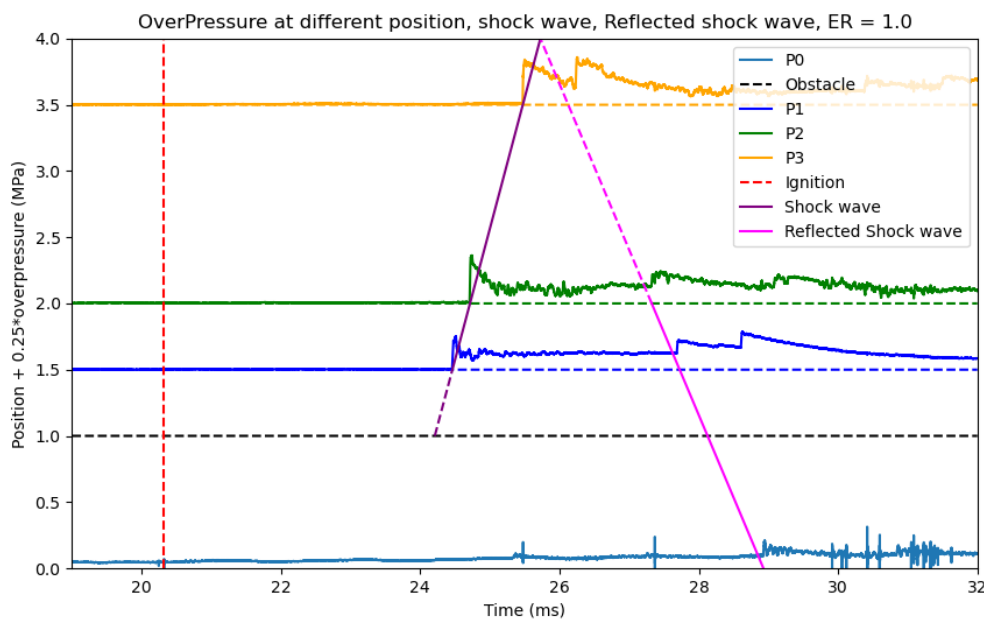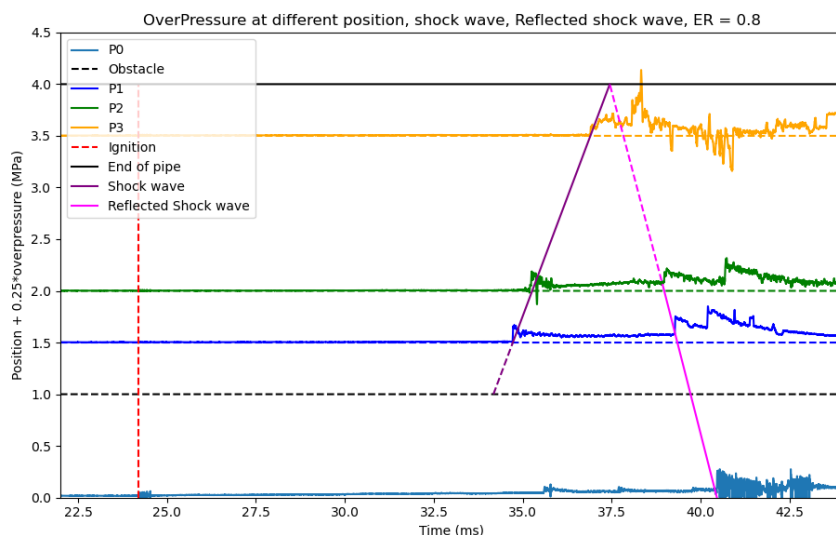

Figure 3.10: Experimental results of overpressure at different positions, shock wave, reflected shock wave, and ignition time at $\varphi = 0.8$ for hydrogen-air mixture explosion in 4m pipe (test no. 25).

The pressure at the end of pipe due to DDT was higher than the reflected pressure at P3, possibly as high as 5 MPa or even more. The sudden increase is due to the confinement of mixture which accelerates the combustion, limits the expansion and the interaction between shock and detonation merging in the end pipe cause the pressure rise. This is the worst-case scenario in DDT and the possibility of damaging the material is high due to the overload. Reflected wave velocity was recorded as 1350 m/s.

3.2.5 Hydrogen-Air Explosion at $\varphi = 0.6$ (20% Hydrogen)

Among the 4 experiments no DDT was observed with an equivalence ratio of 0.6. The pressure response and the wave velocity trend were almost similar in these experiments. In test no. 11 no pressure response was observed in P3 but there was ignition signal in P3 at the same time as P0, P1 and P2. If there was a faulty setting in amplifier or any connection error, there might not be any ignition response in P3. The actual reason for no pressure response in P3 is unknown.

The result of experiment 12 is shown in Figure 3.11. There was an ignition delay of 33.5 ms. The overpressure at P1, P2 and P3 were 0.36 MPa, 0.32 MPa and 0.23 MPa respectively. The wave velocity was recorded as 692 m/s. The cell size varied significantly with ER. In a lean mixture the cell size is higher which means the mixture is less reactive and sensitive to detonation. Larger cell size makes it difficult to accelerate the flame to achieve DDT. As the wave propagated towards the end of the pipe no detonation or DDT was noticed from the pressure response. The maximum reflected overpressure was recorded in P3 as 0.47 MPa which was twice as high than the incident shock wave in the same position. The reason why reflected pressure is higher than the incident is described in $\varphi = 1.0$. The reflection wave had a low velocity. Due to its low velocity when it overcome the velocity of gas mixture behind of it the resultant velocity shows an antilog curvature instead of straight line. Determining the exact velocity from this curve response is difficult but from the travel time between P3 and P1 an approximation of reflected velocity can be found as 851 m/s.
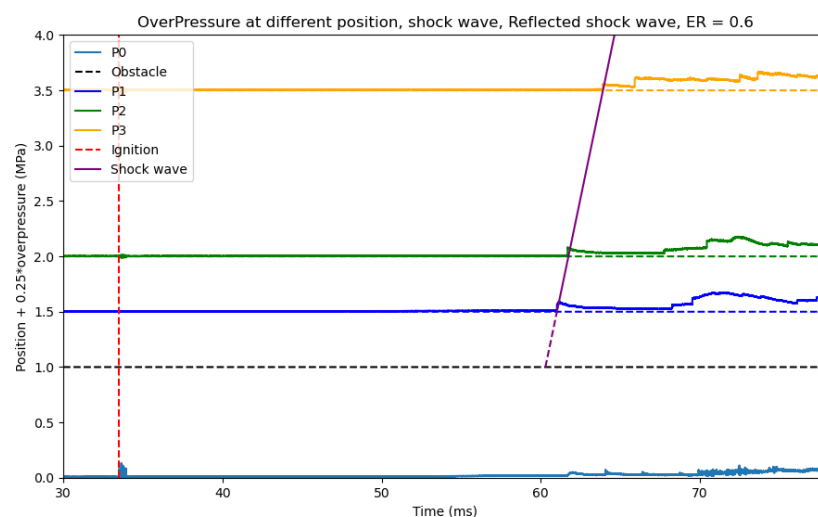

Figure 3.11: Experimental results of overpressure at different positions, shock wave, reflected shock wave, and ignition time at $\varphi = 0.6$ for hydrogen-air mixture explosion in 4m pipe (test no. 12).

3.2.6 Hydrogen-Air Explosion at $\varphi = 1.2$ (33.5% Hydrogen)

DDT was observed in all 4 experiments at $\varphi = 1.2$. Although the wave velocity was almost identical the overpressure response and position of DDT varied throughout the experiments. Maximum overpressure was observed in experiment no. 18 and 28. DDT occurred just after the obstacle in test no. 18, between P1 and P2 in test no. 28. Based on the CJ pressure DDT in test no. 17 and test no. 29 was not cleared. But it seems the DDT lies between P2 and P3 for test no. 17 and between P1 and P2 for test no. 29. The wave velocity ranged from 2039 m/s to 2064 m/s.

Figure 3.12 represents the visual representation of pressure response and wave pattern of experiment 18. Ignition had a time delay of 24.72 ms. Overpressure at P1, P2, and P3 were recorded as 1.85 MPa, 1.40 MPa and 1.41 MPa respectively. Shock wave propagated at a velocity of 2064 m/s. This was the only experiment where transition to detonation occurred just after the obstacle with a maximum overpressure at P1. If the mixture is close to stoichiometric mixture, the cell size is much smaller, and the mixture is more reactive and sensitive. With a minimum turbulence from the obstacle mixture can ignite properly and the shock wave ahead of the mixture travels at higher velocity. In this case, the transition to detonation can happen earlier than lean mixture or rich mixture. Maximum reflected pressure was observed as 1.33 MPa at P3 and the reflected velocity was recorded as 1215 m/s.
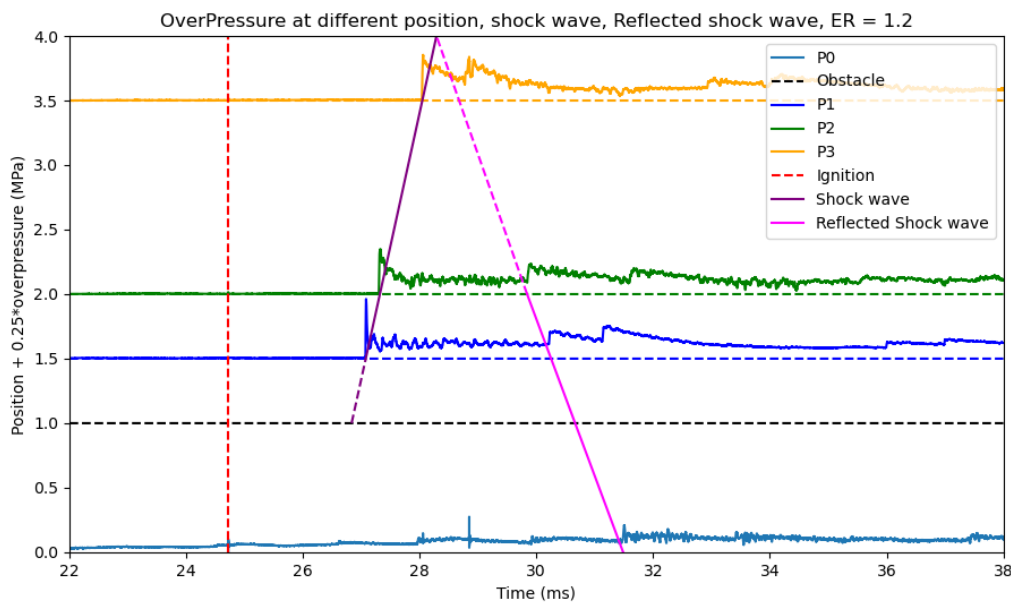
Figure 3.12: Experimental results of overpressure at different positions, shock wave, reflected shock wave, and ignition time at $\varphi = 1.2$ for hydrogen-air mixture explosion in 4m pipe (test no. 18).

3.2.7 CJ Pressure and Experimental Maximum Pressure

The experimental maximum pressure and CJ pressure at different φ is shown in Figure 3.13. The initial atmospheric pressure was added with the overpressure presented in Table 3.1 and the experimental overpressure is turned to pressure in Figure 3.13. In lean mixture the pressure developed due to the wave propagating is much less than the CJ pressure. At $\varphi = 0.8$ only in one experiment experimental pressure is higher than the CJ pressure. But for stoichiometric mixture or slightly rich mixture the experimental pressure is higher than the CJ pressure in most of the experiments. CJ model is a 1D model considering the wave only in

axial direction, however, in real cases the wave propagates in three directions. If the explosion occurs in open place gases can expand freely but in case of confined explosion like pipe wave moving towards the radial direction and increase the pressure. Besides, from the opposite side of the pressure transducers wave moving towards the radial direction reflected and get back to pressure transducers. The prior experiment before $\varphi = 1.0$ and 1.2 was $\varphi = 0.8$ where DDT occurred in the end pipe with higher overpressure and temperature. The initial higher temperature is probably one of the reasons which accelerate the flame propagation and assisting to rapid reaction of the mixtures.
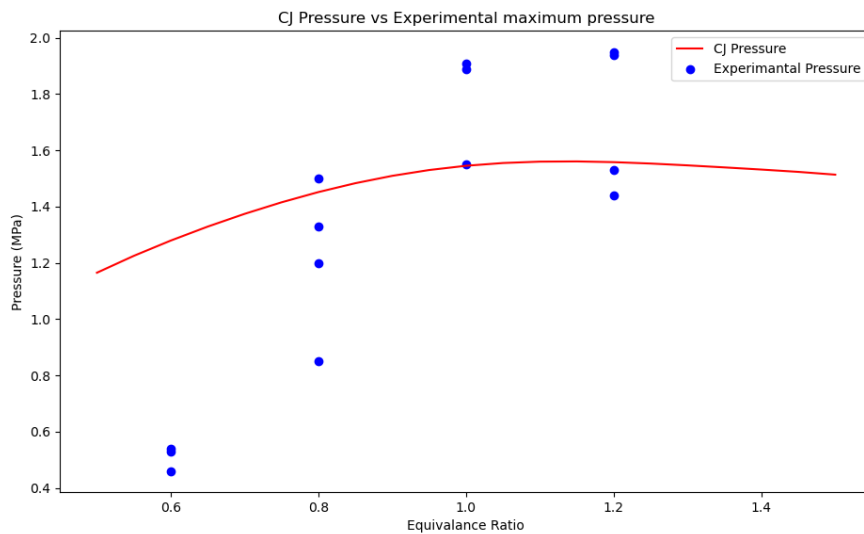
Figure 3.13: Experimental maximum pressure and CJ pressure at different equivalence ratio.

3.2.8 CJ Velocity and Experimental Wave Velocity

The experimental wave velocity and CJ velocity at different φ is shown in Figure 3.14. Experimental wave velocity was much lower than the CJ velocity at $\varphi = 0.6$ and 0.8 (except one experiment). Lean mixtures are less reactive, and the propagation of flame acceleration is lower which produces a low wave infront of the flame. The possibility of direct detonation or DDT in lean mixture is quite low, however, in case of $\varphi = 0.8$ DDT occurred in the end pipe which is much more dangerous than a DDT occurred in the other position of pipe. In the stoichiometric mixture the wave velocity is almost identical to the CJ velocity. A stoichiometric mixture is more reactive and has smaller cell size, propagating the flames at higher velocity creating strong shock wave infront of the flame. In stoichiometric hydrogen air, there is no air or gas remaining after the burning since the combustion is a complete combustion. So, there is no heat loss happen to heat up the unburned air or hydrogen results in acceleration of the flame. A slightly lean or rich mixture can also act as stoichiometric mixture and the wave velocity is close to CJ velocity or even higher. At $\varphi = 1.2$ the experimental wave velocity was little higher than the CJ velocity.
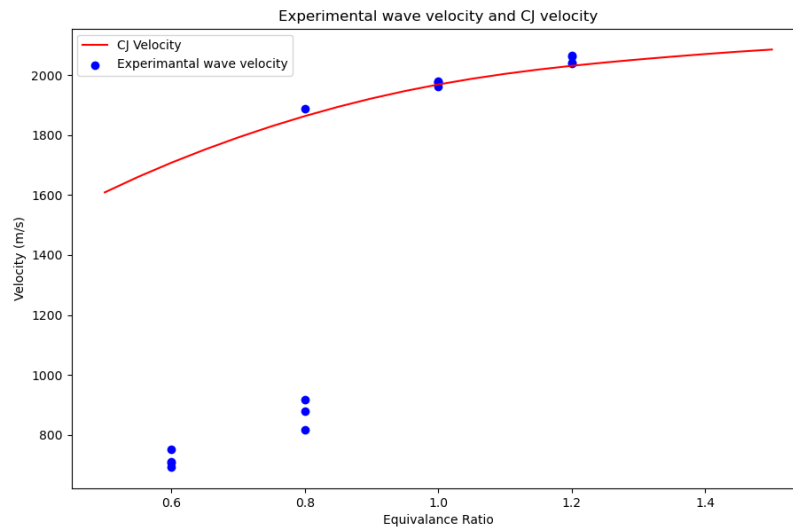
Figure 3.14: Experimental wave velocity and CJ velocity at different equivalence ratio.

For a better visualization Figure 3.15 is also added here.
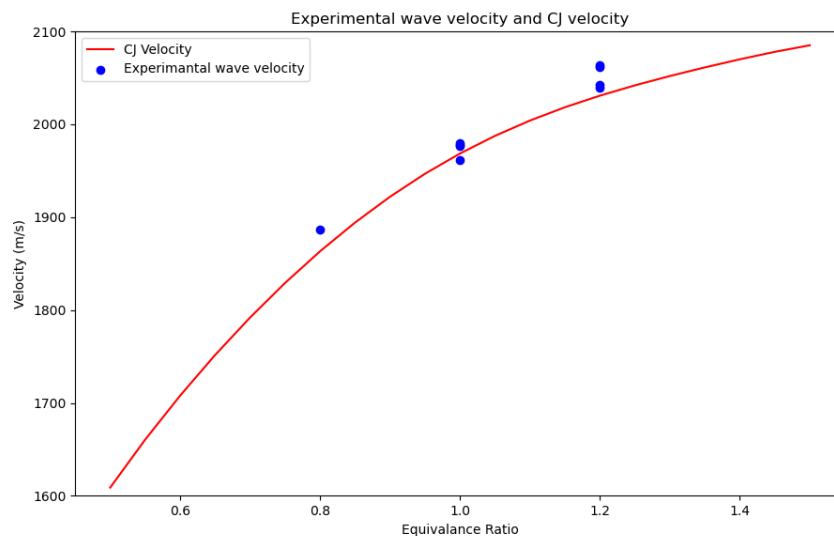
Figure 3.15: Experimental wave velocity and CJ velocity at $\varphi = 1.0$ and 1.2.

3.2.9 Strain Response

Rosette strain gauge was placed in such a way that it's one strain gauge was placed in radial direction, another one in axial direction and other was at 45° between the radial and axial one. After placing the rosette, an approximate deviation of 1° to 2° was noticed. This deviation can be corrected by calculating the principal strain. In this study, the deviation was neglected. More details on principal strain can be found on [40] for this experiments. Equation (3.3) was used to calculate the actual strain from the measured output sensor voltage [42] [43] [44].

$$\varepsilon = \frac{4\ SV}{GF\ \times\ EV} \tag{3.3}$$

Where ε, SV, GF and EV are strain, sensor output voltage, gauge factor and excitation voltage respectively. The value of GF was 2.1 for the strain gauge and EF was 2.5 V in Flexlogger. Figure 3.16 shows the strain result in three directions. The shock wave moving through a pipe is not only a 1D movement but also acts in radial direction. When shock wave propagates in axial direction it also oscillates towards the radial direction. If the shock is too intense the frequency of oscillation as well as the strain will be higher. The deformation in axial direction is low compared with hoop strain and in diagonal direction. When the wave is forced in radial direction it deforms in radial direction immediately and at the same time a low deformation is observed in axial direction. Since the other strain gauge is placed in orthogonal direction of axial and hoop strain the resultants of both this must be higher that's why it slightly higher than radial and axial strain. The frequency of the strain response from the graph is found as 14.6 KHz.
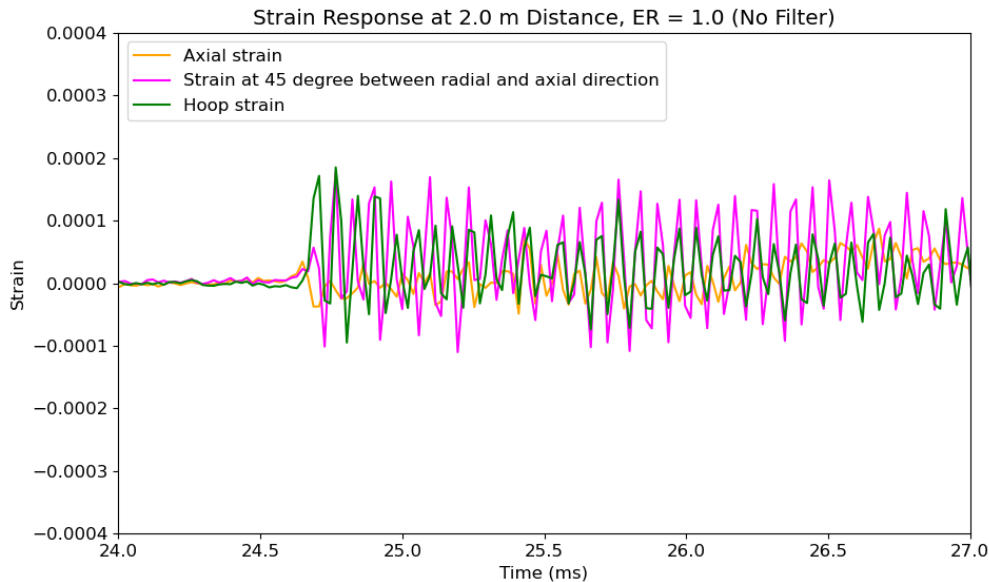
Figure 3.16: Hoop strain, axial strain, and shear strain response in 2.0 m distance at ER 1.0 for experiment no. 16.

Now, from the pressure record hoop strain can be calculated and plot along with the measured hoop strain from strain gauge. Equation (3.4) represents the hoop strain formula calculating from the pressure record.

$$\varepsilon_{hoop} = \frac{PD_i}{2tE} \tag{3.4}$$

ε_{hoop}, P, D_i, t, and E are hoop strain, internal pressure, inner diameter of pipe, thickness of pipe and Young's modulus respectively. The value of E for this material is 210 GPa. The result of simulated hoop strain and measured hoop strain and corresponding pressure is

shown in Figure 3.17. The left side of the vertical axis represents overpressure in MPa, and the right side of the vertical axis represents strain. The hoop strain recorded from the strain gauge showed an early spike compared to the pressure transducer. This is because the wave propagating in metal is much faster than wave propagating in gas mixtures.
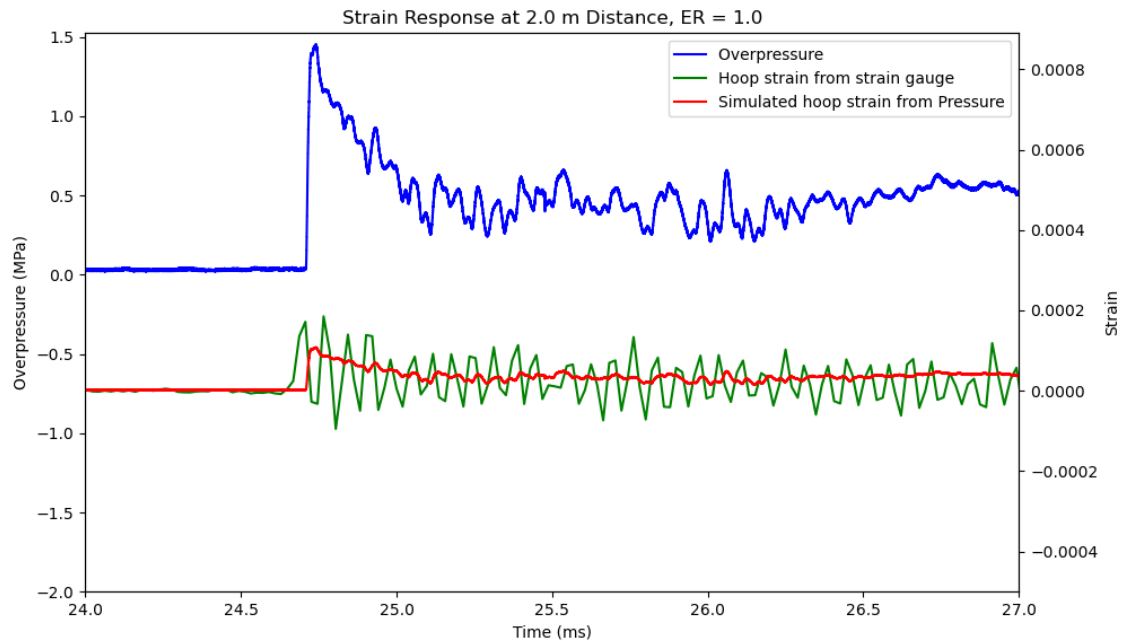
Figure 3.17: Overpressure, hoop strain recorded from strain gauge and hoop strain calculated from internal pressure in 2.0 m distance at ER 1.0 for experiment no. 16.

When the shock wave travels the pressure transducers at 2.0 m, the maximum overpressure was recorded as 1.45 MPa, hoop strain recorded from the strain gauge was 0.000185 and hoop strain calculated from pressure was 0.000111 which gives a dynamic amplification factor of 1.67 between the recorded and calculated hoop strain. From the pressure record inside and using this factor the dynamic hoop strain can be predicted. Beltman et al. experimental results suggest that with a wave velocity of 1978 m/s the experimental DAF is around 1.55 which is shown in Figure 2.9 [20]. Note that Beltman et al. experiment was conducted in a different material tube having different diameter and thickness. However, the strain response and DAF are quite a reasonable agreement with Beltman et al. experiment.

There was no experiment having a velocity close to first critical velocity (1044 m/s) was found to get the maximum DAF.

4 Numerical Simulations

This chapter illustrates a short description on Random choice, Reimann problem, simulation, and comparison with experimental results. Also, represent some prediction based on the simulation.

4.1 Random Choice Method

For nonlinear hyperbolic system a random choice method was illustrated by Chorin [45] which includes the solution of Reimann problem. The method can handle the complex pattern of shock wave and contact discontinuity. A MATLAB version of the method known as RCMLAB was developed by Bjerketvedt et al. at University of South-Eastern Norway (previously known as Telemark University College) [46]. In this study, a modified and preliminary version of RCM in Python is developed for 1D non-stationary unsteady flow of a compressible gas with combustion. A finite volume piecewise constant grid was considered in this method and the local Reimann problem for each cell was solved. Numerical noise was introduced in the smooth waves such as rarefaction waves due to the randomness of the method. However, this problem can be solved by increasing the number of cell computational cells.
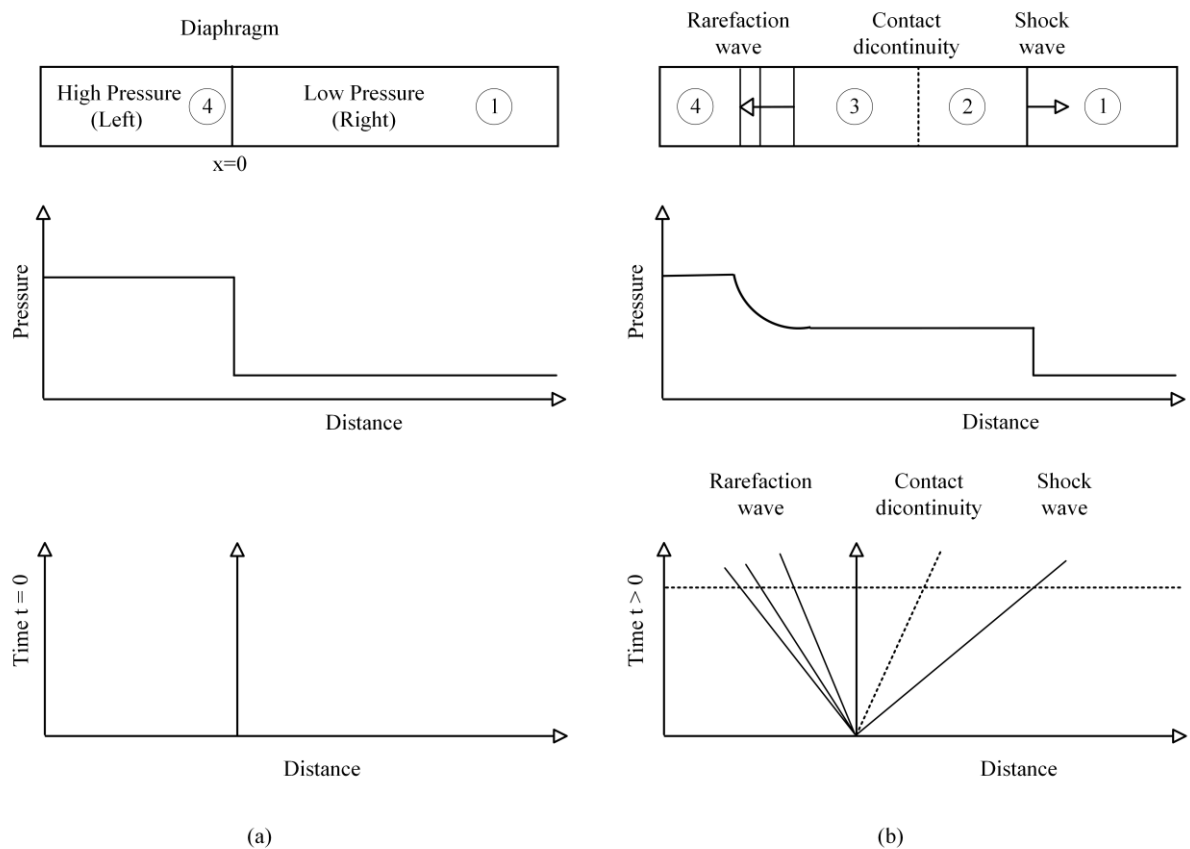

Figure 4.1: (a) Sketch of initial pressure and wave pattern of shock tube and (b) pressure changes and wave propagation after the diaphragm breakdown.

4.1.1 Reimann Problem

Riemann Problem provides fundamental concepts regarding nonlinear hyperbolic systems of partial differential equations (PDEs). It is generalized as a shock tube problem. A long one-dimensional tube (see Figure 4.1) closed from both ends divided into two sections with a diaphragm having different thermodynamic properties (pressure, temperature, and density) in each section is considered. Initially, the gas is at rest, and when the diaphragm breaks down a high-speed compressible flow known as shock wave is propagated towards the lower pressure region. Towards the high-pressure region multiple expansion waves known as rarefaction waves developed. The expanded and compressed gas is separated by a contact discontinuity which travels to the right at a constant speed. At this stage the physical functions (p, ρ, T, U) are discontinuous across the tube. This discontinuity causes difficulty of the problem. The Reimann problem for one-dimensional Euler equation can be written as

$$\frac{\partial \rho}{\partial t} + \frac{\partial(\rho u)}{\partial x} = 0 \tag{5.1}$$

$$\frac{\partial(\rho u)}{\partial t} + \frac{\partial(\rho u^2 + p)}{\partial x} = 0 \tag{5.2}$$

$$\frac{\partial E}{\partial t} + \frac{\partial(u(E + p))}{\partial x} = 0 \tag{5.3}$$

Where ρ, u, t, x, p, E is density, velocity, time, position, pressure, and total energy per unit volume respectively, with the following initial conditions:

$$U(x, 0) = \begin{cases} U_l \ if \ x < 0 \\ U_r \ if \ x > 0 \end{cases}, \qquad where \ U = \begin{matrix} \rho \\ u \\ p \end{matrix} \tag{5.4}$$

The two regions (marked as 2 and 3 in Figure 4.1) between rarefaction wave and shock wave separated by contact discontinuity are known as the star region. In these regions pressure p_*, and velocity u_* are equal but the density ρ_{*l} and ρ_{*r} has different constant value. The state in both right and left are known, and it is necessary to find out the solution in the star region.

In this study, a preliminary version of Reimann solution is used which is in updating form. The more details on Reimann solution can be found in reference [23].

4.2 Simulation Results and Discussions

The RCM described in section 4.1 was used to simulate the pressure response in a 4 m unobstructed open and closed pipe as detonation propagating from one end to another. Initial condition of the simulation was considered as CJ condition. Simulation was done for stoichiometric hydrogen air concentration and a total number of 400 grid cells were considered for 4m length. Figure 4.2 represents 3D plot where the position of pipe, elapse time and corresponding pressure variation is shown in x, y, and z direction respectively. Detonation was considered in the starting of pipe at position 0. This represents the shock

wave, reflected shock wave and the corresponding pressure response in different positions. The initial pressure of the wave at 0 position is 1.57 MPa as CJ pressure. As the wave propagating maximum pressure around 5.7 MPa is obtained at the end of pipe due to the reflection of shock wave. The reason for maximum pressure in the end pipe is described in section 3.2.3. The right view of the figure shows the rarefaction wave as well.

Figure 4.2: Simulated pressure response based on position and time as detonation propagating from one end to another in a 4m closed pipe.

This simulation can also show the density changes over time and position. Figure 4.3 represents a 3D graph where position, time and density are in x, y and z axis respectively. The CJ condition is considered in whole pipe. The initial density at 0 position is around 1.28 kg/m^3. As shock wave propagates towards the end of pipe it compresses the unburned gas mixture in front of it. In the end of pipe maximum compressed gas stored and the density in end pipe is much higher than initial density. The density of the stoichiometric hydrogen air mixture in the end pipe is found to be around 6.5 kg/m^3. When flame reaches the end pipe it creates a high explosion because there is a high concentrated mixture in the end pipe which results in a high explosion pressure in the end.
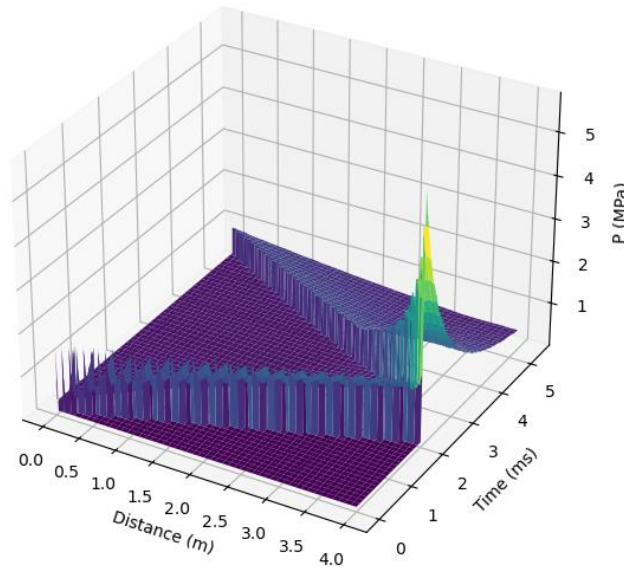
Figure 4.3: Simulated density response based on position and time as detonation propagating from one end to another in a 4m closed pipe.

4.2.1 Experimental and Simulated Pressure

In the initial development of RCM in python obstacle is not considered. Since the distance between obstacle and the pipe end was 3m, simulation was considered for 3m to compare with experimental result. Experiment 26 and simulation pressure for 3m closed pipe is shown in Figure 4.4. Atmospheric pressure is added with the overpressure of experiment. In case of simulation detonation was considered exactly in the obstacle position, however, in experiment actual detonation occurred closed to 1 m away from the obstacle and that's why the simulated pressure response at position 1.5 m is higher than the experimental result. At position 2.0 m experimental pressure was approximately 0.22 MPa higher than the simulated pressure. Due to the expansion wave behind the shock, there is a gradual decrease in pressure. The second pressure rise in the pressure transducers is because of the shock wave reflected from the end wall approximately at 2 ms. Simulated expansion wave is slightly lower than the experimental result. The second pressure response due to the end wall reflection is quite align with the experimental value in terms of pressure reading and the timing as well. As the reflected wave travels towards the obstacle, it reflected again, and the 3rd pressure rises because of the reflection from the obstacle. In case of experiment reflection happened from the obstacle blockage section only, however, in simulation it was considered as complete closed end. Pressure response of a reflection wave from a closed end is always higher than a partly closed end. Besides, the simulation showed less noise compared with the experimental value.

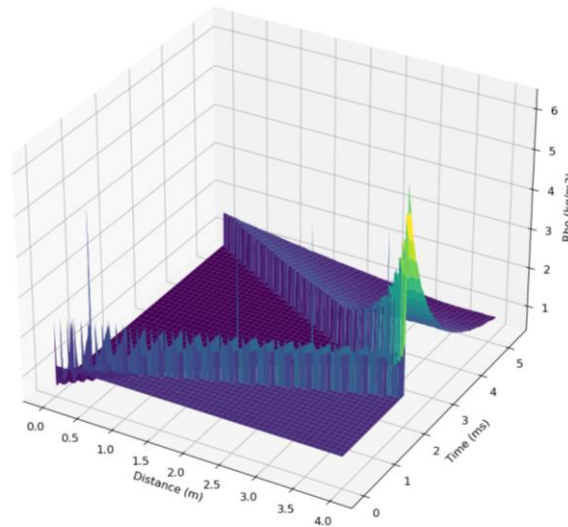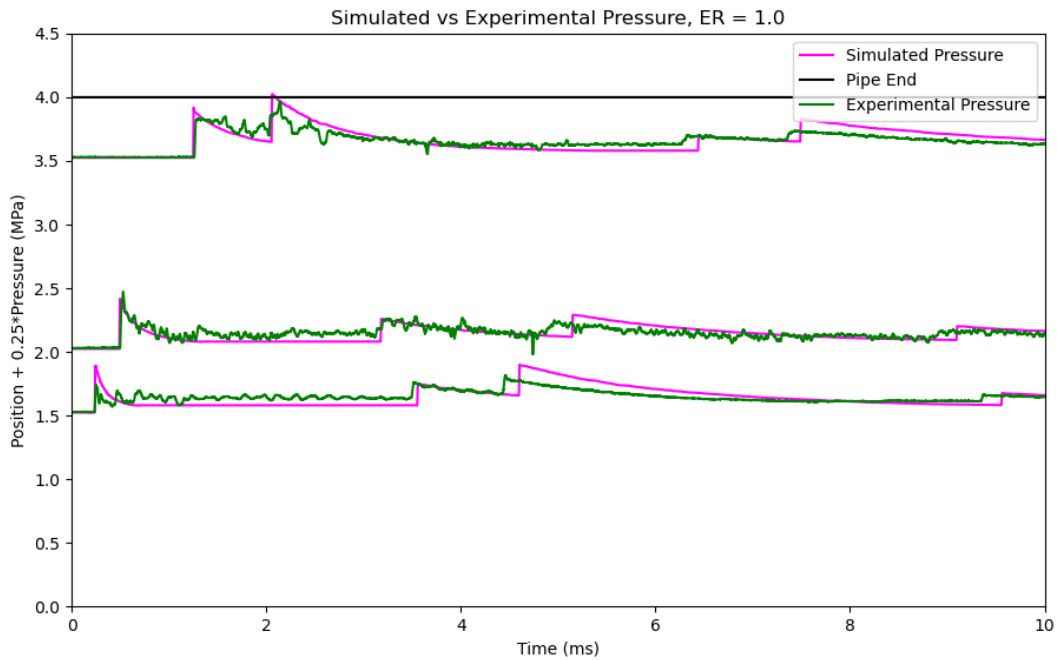Figure 4.4: Simulated and experimental (test no. 26) pressure response based on position and time as detonation propagating from one end to another in a 4m closed pipe.

4.2.2 Load Prediction with RCM

In experiments 13, 14 and 24 at $\varphi = 0.8$ DDT occurred in the end pipe and the maximum reflected overpressure at P3 was observed as 2.56 MPa. The position of P3 was 0.5 m apart from the end wall. Pressure at the end wall must be higher than the reflected pressure at P3. RCM pressure in the end wall can be predicted by considering the detonation at the end pipe. The CJ condition is considered in the whole pipe. Initial pressure at the beginning is CJ-pressure for this simulation. In real cases this pressure might be varied. Figure 4.5 shows the pressure response due to detonation in the end pipe at $\varphi = 1.0$. Maximum pressure is found as 5.7 MPa while it was found as 5.23 MPa using detonation toolbox [18].
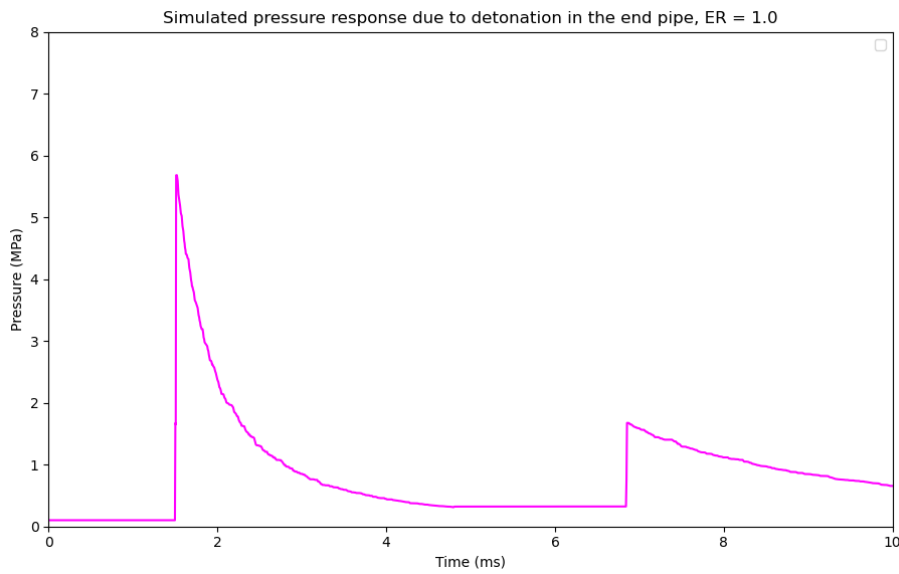
Figure 4.5: Simulated pressure response due to detonation in the end pipe at $\varphi = 1.0$.

A simulation was performed for a 50 m open pipe and pressure response at different positions is shown as Figure 4.6. The pressure is multiplied by 2. Detonation was considered at the 0 position of the pipe. The pressure throughout the pipe is found as 1.67 MPa, however, in case of closed pipe the simulated pressure in the end pipe is 5.7 MPa.
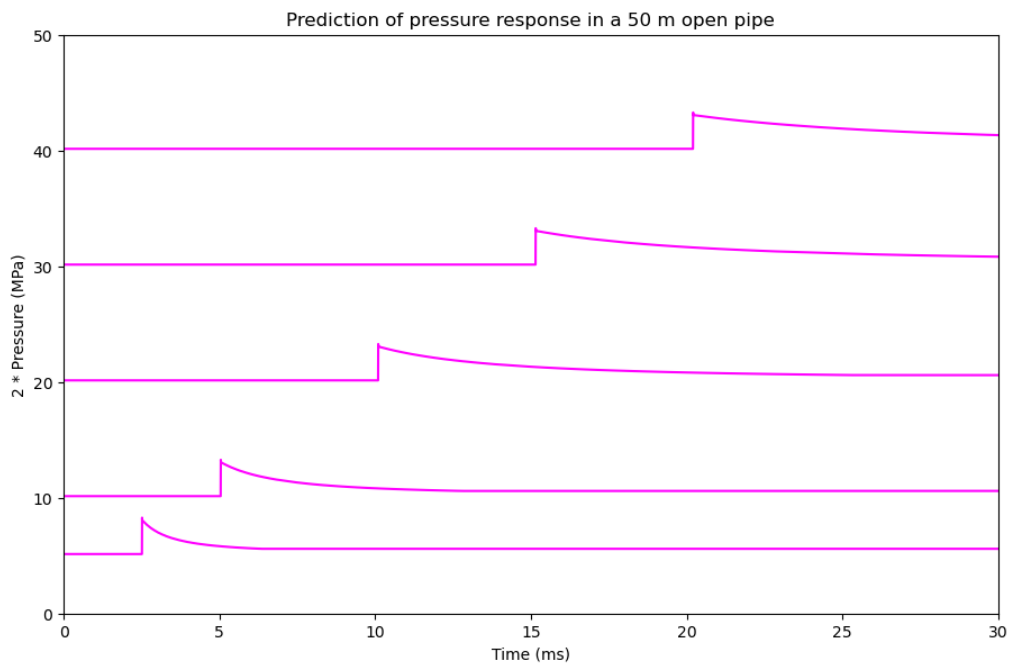
Figure 4.6: Prediction of pressure response in a 50 m open pipe at ER 1.0.

The RCM is in good agreement with experimental result, but it is a preliminary version. Further development is necessary for improvement.

5 Discussions

This chapter describes possible uncertainty in experiments, summary of findings, possibility of implementing a vent system and some recommendations for future work.

5.1 Possible Uncertainty

- Commercially graded hydrogen gas is very pure with purity greater than 99.9 % or even more. So, the possible uncertainty was the mixing of hydrogen with air. Hydrogen flow control was measured in kg/hr while the air flow was measured in g/s. For a stoichiometric mixture hydrogen flow rate was 30 kg/hr and air flow rate was 287 g/s. In the case of hydrogen flow rate VAFM reading didn't show the fraction value. When the actual flowrate was greater than 29.50 to 30.49 kg/hr VAFM showed it as 30 kg/hr. So, a deviation of hydrogen flowrate $\pm$ 0.49kg/hr (equivalent to ER $\pm$ 0.016) was one of the possible errors in gas mixtures. Besides, when the air compressor refill by itself a sudden fall just before the filling and rise after the filling was noticed. It deviates the flowrate $\pm$ 8 g/s. This is one of the possible reasons that in experiment 25 at ER 0.8 DDT occurred between P1 and P2 instead of end pipe.

- The time delay between explosions was approximately 20 to 30 minutes throughout the experiments and it was noticed that after a few explosions the pipe became heated. Although only air was supplied for 5 to 10 minutes for flashing after every explosion it was not enough to return the temperature to the initial temperature. The outlet valve was closed after 1 minute from the closing of inlet valve to settle down the inside pressure to atmospheric condition. But for a high inflow rate gas mixture, a small nozzle opened for 1 minute may not be enough to reduce the pressure to atmospheric pressure. Besides, if the outlet valve is kept opened for a longer period there is a high possibility of air entering the pipe and resulting in a leaner mixture. The initial pressure and temperature of a combustible mixture has a great influence on burning velocity, flame quenching, flame thickness, sound speed and a significant variations in critical run-up distances [31]. Experiment 25 was the 6th experiment on that day. The prior experiment 24 had a detonation in the end pipe with a high pressure rise and so does high temperature. The initial temperature might have been higher than the room temperature for experiment 25 caused to early DDT. Variation in temperature cause thermal expansion in strain and also influence the resistance of the gauge [42].

- From the static pressure test results leakage was noticed in the pipe. If there is a leakage there is a possibility of air entering the pipe making a leaner mixture. For the same flow rate, a similar pressure reading was expected from all pressure transducers, but it shows a different reading. However, the pressure trend was the same. The pressure transducers are several years old. So, there is a possibility of mismatch between the actual pressure vs the pressure recorded by transducers.

- Noise was noticed in the data acquisition especially for NI instruments. The high voltage ignition source was one of the possible reasons for this noise. High voltage ignition source can create a high electromagnetic interference which affects electronic instruments like strain gauge [42]. Rapid change in current creates an unexpected

voltage change in the strain gauge known as noise. Besides, normal electrical wire was not shielded and any electromagnetic interference from the surroundings can create noise.

- After a few experiments a permanent deformation in strain gauge S0 was noticed. After this deformation strain gauge continuously demonstrated negative response in all three directions. The strain gauge placing in the end pipe showed a high strain in 45° angle between radial and axial direction while the radial strain was quite low throughout the experiments. Even pressure calculation was done with the hoop strain formula the pressure was lower than the pressure recorded at 0.5 m away from the end pipe.

- Flanges, clamps, and obstacles are the major boundary conditions which might affect the free oscillation of pipe, but it wasn't considered during strain calculation.

5.2 Summary of Findings

- **Instruments:** PicoScope has better data acquisition compared with NI instruments in terms of signal noise. It may be possible to improve the NI data acquisition by changing the electrical wire to highly efficient shielded signal wire. Also, it can be possible to connect the strain gauge to PicoScope which can reduce the noise. Further research can be done to come up with a solution. Besides, there is a possibility of permanent deformation in strain gauges, and it was noticed both in S0 and S2 strain gauges. From the static pressure response, it was noticed that there was leakage in the pipe. It was also noticed that for a constant flowrate the pressure transducers showed a different reading. It means the reading of pressure transducers may not be precise.
- **Sampling rate:** In a closer look to Figure 3.15 it is noticed that the wave pattern in pressure is smooth mostly sinusoidal where the wave pattern in strain represents peak and trough only. In some cases, the peak or trough is flattened, for example, at 24.9 ms the peak is flattened. For a complete cycle at least 2 samples should be taken in order to not lose the peak and trough, however, there is a possibility of flattening the peak and trough. From the strain record the frequency was found as 14.6 KHz and the sampling rate was 30 KHz. It can be said that the data acquisition was optimum for strain gauge, however, with a higher sampling rate the acquisition will be more accurate and there will be no risk of loosening the peak and trough. With a higher sampling rate, the wave pattern will be sinusoidal that is expected in case of strain response. It's difficult to say the exact optimum sampling rate, however, a sampling rate of 10 times greater than the frequency of wave will ensure an expected wave pattern along with peak and trough in every cycle.
- **Experimental results:** Mixture compositions greatly influence the DDT, run-up distance, wave velocity and pressure response. Early DDT was observed in stoichiometric ratio and the run-up distance was 1.5 to 2.0 m. The cell size is minimum in stoichiometric ratio and the mixture is more reactive which assists to develop early DDT. In case of very lean mixture (φ is around 0.6 or less) there is no possibility of detonation and DDT, however, for slight lean mixtures (φ is around 0.8) for a closed pipe DDT occurred in the end pipe. This is the most dangerous event which developed the maximum overpressure. In these experiments 2.56 MPa reflected

overpressure was recorded at 3.5 m distance when DDT occurred in the end pipe. For rich mixtures at $\varphi = 1.2$ the run-up distances varied where in one experiment it was 1.0 to 1.5 m and 1.5 to 2.0 m in another experiment. In the case of the remaining two experiments from the pressure response the DDT was uncleared. It can be concluded that in terms of mixture composition DDT mostly depends on moderate lean mixtures at $\varphi = 0.75$ (possibly little less or high as well) to rich mixtures. In the case of closed pipe, a slight lean mixture is the most dangerous one since the DDT occurred in end pipe with high temperature. The detonation wave velocity was quite aligned with the CJ velocity in stoichiometric and at $\varphi = 1.2$. For a DDT in stoichiometric and ER the maximum recorded overpressure was higher than the CJ pressure. The CJ model is one dimensional while the actual scenario of confined pipe is three dimensional. Due to the movement of wave in the radial direction and reflected wave from the opposite of pressure transducers recorded pressure is higher than CJ pressure.

Compared with axial strain the radial strain was higher. When the wave propagating in axial it can induce additional strain when it gets reflected from the end but in case of radial it gets reflected from the opposite side and the strain is higher. Besides, the hoop strain can be predicted from the internal pressure record. However, the factors between predicted hoop strain to recorded hoop strain might be varied. Strain in end pipe must be higher both in axial and radial direction due to the high pressure and reflection from end wall. However, unfortunately the strain gauge placed in the end didn't work. Further research can reveal the response.

- **Numerical Simulation:** The numerical simulation in RCM developed in python is in its early stages. Simulated and experimental pressure response were in good agreement. Obstacle was not included in the simulation yet that's why the simulation was done for 3m to compare with experimental results. In the case of experiments DDT occurred between 0.5 to 1.0 m away from obstacle, however, in simulation detonation considered in the 0 position. With simulation detonation in the end pipe gives 5.7 MPa pressure. In the case of experiments with end pipe DDT reflected overpressure at 0.5 m away from the end pipe was measured as 2.56 MPa. It can be predicted that the induced pressure might be around 5.0 MPa. In simulation the pressure measured from detonation in end pipe while in experiments pressure recorded was from DDT in end pipe.

5.3 Factors Need to be Consider Implementing a Hydrogen Emergency Vent System

Since the DDT phenomenon is quite sophisticated and depends on multiple factors, implementing a complete risk-free vent system is quite difficult. However, from this experiment and different literature an overview can be illustrated to implement a hydrogen emergency vent system.

- **The materials of the pipes and pressure relief valve or rupture disk should be low electricity conductive, high convection heat transfer coefficient and low roughness coefficient:** Since hydrogen has a very low ignition energy a minimum spark from the metal can induce combustion easily. So, a metal with low electric conductive can be better to avoid ignition. Due to the high flow rate inside the pipe internal temperature increases and there is a risk of auto-ignition. If the material has a

high convection heat transfer coefficient it can release the increased temperature to the surroundings and there will be no risk of auto ignition. Even if any ignition occurred high convective material can assist to quench the flame and reduce the risk of flame acceleration and DDT. The roughness of the pipe has a great influence on turbulent flow and so does the flame acceleration and transition to DDT. Material with low roughness coefficient will be highly effective to keep the flow smooth.

- **The whole system should be leaked tight and unobstructed:** From the experimental result of this study, it is found that there is a risk of detonation or DDT from a moderate lean mixture to a rich mixture including stoichiometric. Basically, this φ ranges from 0.75 (maybe little low or high as well) to rich mixtures. Leaks in pipe allow air intrusion creating a combustible mixture and from one of the possible ignition sources it can be ignited. The turbulent flow of the gas mixture is the most sensitive term in case of flame acceleration, detonation, and DDT in explosion. Any resistance (obstacle, pipe joint, elbow, tee etc.) in the smoothen flow can create turbulence. In industrial application completely avoiding this is not possible but reducing elbow, tee and other structure which cause the turbulence flow will reduce the risk. The onset of DDT mostly relies on the position where turbulent flow is developed or little far away. So, the pipe elbow, tee, joint as well as some distance of the pipe material after and before of this should be stronger than the other parts.

- **Clogging of vent stack and flow rate should be considered:** Clogging in vent system creates a significant safety risk. Clogging mainly occurred due to ice formation, intrusion of foreign material and lack of maintenance for a long time. If clogging happens the whole pipe acts as a closed pipe and pressure develops inside of the pipe until the pressure difference between pipe and storage is zero. The vent system should overcome this pressure. The most devastating situation will occur if an explosion happens with this pressure build situation. With a high pressure the hydrogen is more compressed and highly dense. So, the maximum pressure builds up based on the flow rate and internal pressure of the storage should be taken into account. If an explosion happens and DDT occurs at the end of pipe very high pressure will develop. A high strength material can be used in the end part of the pipe, and it must be very low electric conductive since the hydrogen venting from the end pipe mixes with air.

- **Initial conditions:** From detonation toolbox it is found that a rise of initial pressure from 0.1 MPa to 0.5 MPa increase the CJ pressure from 1.55 MPa to 7.91 MPa for a stoichiometric hydrogen air combustion [18]. When hydrogen moves at a high flowrate the pressure inside the pipe is higher than atmospheric pressure and if the pipe ends clogged then the inside pressure will be much higher. Before designing the vent system, the maximum pressure that can be developed from the flowrate needs to be considered.

- **Pressure relief valve or rupture disk:** Pressure relief valve opens when the internal pressure of the storage exceeds a predetermined level and closes again when the internal pressure is reduced to its safe zone. It ensures limiting the vent of hydrogen and the risk of failure is low. In case of rupture disk, the disk will rupture if the internal pressure exceeds a predetermined level, and the flow will continue until the pressure between outside and inside of the storage is equal. In terms of safety consideration and reducing the loss of hydrogen, pressure relief valve may be a better choice than the rupture disk.

5.4 Recommendations

- The initial pressure and temperature have a great influence on flame acceleration, run-up distance, detonation, and DDT. Further research by changing this parameter will reveal the effect of initial conditions.
- Acceleration of flame is higher in long and open pipe. Since the vent pipe is long and open an experimental study on long and open pipe can be done.
- Although obstacles induce turbulence and flame acceleration, the pipe elbow, tee, and other joint might have different response in flame acceleration and DDT. A study on placing different elbows can be done to investigate the response.
- For a better wave pattern and ensure no loosening of peak and trough a sampling rate of 0.15 MHz (10 times greater than strain frequency) or more is recommended.
- The result of the end pipe strain gauge was unexpected (described in section 5.1). Since the highest pressure develops in the end pipe, the strain response in the end pipe is necessary. Placing a new rosette strain gauge as well as single directed strain gauge will find out the uncertainty of strain response in end pipe.
- In industrial hydrogen release the mixture is not homogenous and from the review there is a mixed conception about inhomogeneous mixture. A further experimental study on inhomogeneous mixture can reveal the real scenario.
- Since there was no wave velocity was found close to first critical velocity (1044 m/s) more experiments with hydrogen concentration 25 to 29 % can be done to get this velocity and observe the maximum DAF.
- Obstacles, elbow, tee, and other pipe joints can be included in the numerical simulation which will be effective to predict the actual scenario of hydrogen explosion.
- The deformation of pipe can be illustrated from the internal pressure response by Finite Element Analysis.

6 Conclusion

To find out the possible structural load hydrogen -air explosions at different concentrations in a 4 m pipe was conducted placing an obstacle 1m away. Four pressure transducers and three rosette strain gauges were placed in the pipe to record pressure and strain response. The Equivalence Ratio of hydrogen-air mixtures consider as 0.6, 0.8 ,1.0 and 1.2. No DDT was observed in $\varphi = 0.6$. At stoichiometric and $\varphi = 1.2$ DDT was observed since the cell size in stoichiometric and rich mixture is minimum which ensures a more reactive mixture. Concentration greatly influences the run-up distance. The run-up distance is minimum if the mixture is stoichiometric or little rich mixture. DDT was observed in the end of pipe in case of $\varphi = 0.8$ which demonstrated maximum reflected overpressure of 2.56 MPa at 3.5 m distance. Then the pressure in the end pipe might be as high as 5 MPa or even more. A DDT in the end pipe is much more dangerous than a DDT in the other position of pipe. It can be said that an Equivalence Ratio ranges from 0.75 (possibly little low or high) to rich mixtures are the critical concentrations for DDT development. The experimental pressure was mostly higher than the CJ pressure in the case of DDT experiments. It is because the CJ model is 1D and the actual scenario is 3D where the additional load comes from the oscillation of wave in radial direction. The wave velocity in DDT experiments and corresponding CJ velocity were in good agreement. From the rosette strain gauge high strain was noticed in the orthogonal of radial and axial direction of pipe. In 2.0 m distance of pipe a dynamic amplification factor of 1.67 was found between the recorded hoop strain from strain gauge and the calculated hoop strain from internal pressure record at $\varphi = 1.0$.

From the random choice method numerical simulation, it is also found that the pressure showed a similar response with experimental recorded pressure. The numerical simulation is in the early stages. It is found that a pressure of 5.7 MPa can be developed if the detonation occurred in the end pipe. With this code the pressure response both in open and closed pipe can be predicted.

References

[1] Y. Du, Y. Liu, F. Zhou, L. Li, J. Zhang, and Z. Zhang, "Propagation and intensity of blast wave from hydrogen pipe rupture due to internal detonation," *J. Loss Prev. Process Ind.*, vol. 81, p. 104933, Feb. 2023, doi: 10.1016/j.jlp.2022.104933.

[2] W. I. Inc, "Case Study: Power Plant Hydrogen Explosion," WHA International, Inc. Accessed: Mar. 08, 2024. [Online]. Available: https://wha-international.com/case-study-power-plant-hydrogen-explosion/

[3] D. Bjerketvedt, J. R. Bakke, and K. Van Wingerden, "Gas explosion handbook," *J. Hazard. Mater.*, vol. 52, no. 1, pp. 1–150, Jan. 1997, doi: 10.1016/S0304-3894(97)81620-2.

[4] C. San Marchi, A. Harris, M. Yip, B. P. Somerday, and K. A. Nibur, "Pressure Cycling of Steel Pressure Vessels With Gaseous Hydrogen," presented at the ASME 2012 Pressure Vessels and Piping Conference, American Society of Mechanical Engineers Digital Collection, Aug. 2013, pp. 835–844. doi: 10.1115/PVP2012-78709.

[5] "EPSC - European Process Safety Centre - EPSC Learning Sheets." Accessed: Apr. 25, 2024. [Online]. Available: https://epsc.be/Learning+Sheets/EPSC+Learning+Sheets.html

[6] "DOC211-hydrogen safety," studylib.net. Accessed: Apr. 12, 2024. [Online]. Available: https://studylib.net/doc/27112184/doc211-hydrogen-safety

[7] V. Knudsen, "Hydrogen gas explosions in pipelines - modeling and experimental investigations".

[8] S. McAllister, J.-Y. Chen, and A. C. Fernandez-Pello, *Fundamentals of Combustion Process*.

[9] S. KI, "Influence of tube roughness on the formation and detonation propagation in gas," *J. Exp. Theor. Phys.*, vol. 10.10 (1940):, pp. 823-827..

[10] S. B. Dorofeev, "Flame acceleration and explosion safety applications," *Proc. Combust. Inst.*, vol. 33, no. 2, pp. 2161–2175, 2011, doi: 10.1016/j.proci.2010.09.008.

[11] E. O. C. de C, "Flame movement in gaseous explosive mixtures," *J. Fuel Sci.*, vol. 7, pp. 502–508, 1928.

[12] C. Clanet and G. Searby, "On the 'tulip flame' phenomenon," *Combust. Flame*, vol. 105, no. 1, pp. 225–238, Apr. 1996, doi: 10.1016/0010-2180(95)00195-6.

[13] Ciccarelli, G, *Combustion Course Notes*. Kingston, Queen's University.

[14] D. Bjerketvedt, "Combustion and Process Safety Course." University of South-Eastern Norway, 2022.

[15] C. M. Guirao, R. Knystautas, J. H. Lee, W. Benedick, and M. Berman, "Hydrogen-air detonations," *Symp. Int. Combust.*, vol. 19, no. 1, pp. 583–590, Jan. 1982, doi: 10.1016/S0082-0784(82)80232-4.

[16] W. Rakotoarison, A. Pekalski, and M. I. Radulescu, "Detonation transition criteria from the interaction of supersonic shock-flame complexes with different shaped obstacles," *J. Loss Prev. Process Ind.*, vol. 64, p. 103963, Mar. 2020, doi: 10.1016/j.jlp.2019.103963.

[17]   K. Aizawa *et al.*, "Study of detonation initiation in hydrogen/air flow," *Shock Waves*, vol. 18, no. 4, pp. 299–305, Sep. 2008, doi: 10.1007/s00193-008-0166-6.

[18]   "Explosion Dynamics Laboratory." Accessed: Mar. 29, 2024. [Online]. Available: https://shepherd.caltech.edu/EDL/PublicResources/sdt/

[19]   R. D. Blevins, *Formulas for natural frequency and mode shape*. New York : Van Nostrand Reinhold Co., 1979. Accessed: May 14, 2024. [Online]. Available: http://archive.org/details/formulasfornatur0000blev

[20]   W. M. Beltman and J. E. Shepherd, "LINEAR ELASTIC RESPONSE OF TUBES TO INTERNAL DETONATION LOADING," *J. Sound Vib.*, vol. 252, no. 4, pp. 617–655, May 2002, doi: 10.1006/jsvi.2001.4039.

[21]   T. Simkins, "Resonance of exural waves in gun tubes." Tech. Rep. ARCCBTR 87008, US Army Armament Research, Develop ment and Engineering Center, Watervliet, N.Y. 121894050., 1987.

[22]   J. E. Shepherd, "Structural Response of Piping to Internal Gas Detonation," *J. Press. Vessel Technol.*, vol. 131, no. 3, p. 031204, Jun. 2009, doi: 10.1115/1.3089497.

[23]   V. Knudsen, "Hydrogen gas explosions in pipelines - modeling and experimental investigations," 2006. Accessed: Mar. 08, 2024. [Online]. Available: https://www.semanticscholar.org/paper/Hydrogen-gas-explosions-in-pipelines-modeling-and-Knudsen/1f272179517d32222cb7860e65115ee0671fbbf0

[24]   K. Wingerden, D. Bjerketvedt, and J. R. Bakke, "Detonations in pipes and in the open," Accessed: Mar. 08, 2024. [Online]. Available: https://www.semanticscholar.org/paper/Detonations-in-pipes-and-in-the-open-Wingerden-Bjerketvedt/9351fa746bffeac3df8ada0b0cead6e3264c930d

[25]   S. Z. Sulaiman, R. M. Kasmani, A. Mustafa, and R. Mohsin, "Effect of Obstacle on Deflagration to Detonation Transition (DDT) in Closed Pipe or Channel–An Overview," *J. Teknol.*, vol. 66, no. 1, Dec. 2013, doi: 10.11113/jt.v66.1326.

[26]   M. Henriksen, D. Bjerketvedt, and K. Vaagsaether, *Deflagration-to Detonation Transition of Hydrogen-Air Mixture in a Highly Congested, Open-ended Channel*. 2022.

[27]   J. Keilers, "Structural Effects of Postulated Hydrogen Explosions in Process Piping and Vessels - 20274," WM Symposia, Inc., PO Box 27646, 85285-7646 Tempe, AZ (United States), INIS-US-21-WM-20274, Jul. 2020. Accessed: Mar. 08, 2024. [Online]. Available: https://www.osti.gov/biblio/23030461

[28]   A. V. Gaathaug, "Experimental Study of Deflagration to Detonation Transition in Hydrogen-Air Mixtures".

[29]   M. Kuznetsov, V. Alekseev, · Matsukov, and · Dorofeev, "DDT in a smooth tube filled with a hydrogen-oxygen mixture," *Shock Waves*, vol. 14, pp. 205–215, Jan. 2005.

[30]   S. Maeda, M. Fujisawa, S. Ienaga, K. Hirahara, and T. Obara, "Effect of sandpaper-like small wall roughness on deflagration-to-detonation transition in a hydrogen–oxygen mixture," *Proc. Combust. Inst.*, vol. 37, no. 3, pp. 3609–3616, 2019, doi: 10.1016/j.proci.2018.07.119.

[31]   S. B. Dorofeev, "Hydrogen flames in tubes: Critical run-up distances," *Int. J. Hydrog. Energy*, vol. 34, no. 14, pp. 5832–5837, Jul. 2009, doi: 10.1016/j.ijhydene.2009.01.008.

[32]   R. Blanchard, D. Arndt, R. Grätz, M. Poli, and S. Scheider, "Explosions in closed pipes containing baffles and 90 degree bends," *J. Loss Prev. Process Ind.*, vol. 23, no. 2, pp. 253–259, Mar. 2010, doi: 10.1016/j.jlp.2009.09.004.

[33]   K. G. Vollmer, F. Ettner, and T. Sattelmayer, "Deflagration-to-Detonation Transition in Hydrogen/Air Mixtures with a Concentration Gradient," *Combust. Sci. Technol.*, vol. 184, no. 10–11, pp. 1903–1915, Oct. 2012, doi: 10.1080/00102202.2012.690652.

[34]   Z. Yin *et al.*, "Effects of Obstacles on Deflagration-to-Detonation Transition in Linked Vessels," *Combust. Sci. Technol.*, vol. 194, no. 6, pp. 1265–1281, Apr. 2022, doi: 10.1080/00102202.2020.1810679.

[35]   D. R. White, "On the existence of higher than normal detonation pressures," *J. Fluid Mech.*, vol. 2, no. 5, pp. 513–514, Jul. 1957, doi: 10.1017/S0022112057000300.

[36]   T. W. Chao and J. E. Shepherd, "Comparison of fracture response of preflawed tubes under internal static and detonation loading," *J. Press. Vessel Technol. Trans. ASME*, vol. 126, no. 3, pp. 345–353, 2004, doi: 10.1115/1.1767861.

[37]   Y. Du, F. Zhou, W. Hu, L. Zheng, L. Ma, and J. Zheng, "Incremental dynamic crack propagation of pipe subjected to internal gaseous detonation," *Int. J. Impact Eng.*, vol. 142, p. 103580, Aug. 2020, doi: 10.1016/j.ijimpeng.2020.103580.

[38]   L. R. Boeck, J. Hasslberger, F. Ettner, and T. Sattelmayer, "Investigation of Peak Pressures During Explosive Combustion of Inhomogeneous Hydrogen-Air Mixtures," in *Proceedings of the Seventh International Seminar Fire and Explosion Hazards*, Research Publishing Services, 2013, pp. 959–965. doi: 10.3850/978-981-07-5936-0_14-09.

[39]   "Pressure sensors | Kistler." Accessed: May 09, 2024. [Online]. Available: https://www.kistler.com/INT/en/c/pressure-sensors/CG21-pressure-sensors

[40]   I. N. N. Solomon, "Structural Response due to Detonation in Hydrogen Emergency Vent Systems." Master's thesis-2024, University of South-Eastern Norway.

[41]   "Test and Measurement Systems, a part of Emerson." Accessed: May 13, 2024. [Online]. Available: https://www.ni.com/en.html

[42]   "Strain gauge," *Wikipedia*. Mar. 11, 2024. Accessed: Apr. 22, 2024. [Online]. Available: https://en.wikipedia.org/w/index.php?title=Strain_gauge&oldid=1213117069

[43]   "Basics of Strain Measurement | Strain Measurement | DAQ Instrument Basics | KEYENCE America." Accessed: May 02, 2024. [Online]. Available: https://www.keyence.com/ss/products/daq/lab/strain/measurement.jsp

[44]   "Introduction to Strain Gauges." Accessed: May 02, 2024. [Online]. Available: https://community.sw.siemens.com/s/article/Introduction-to-Strain-Gauges

[45]   J. Glimm, "Solutions in the large for nonlinear hyperbolic systems of equations," *Commun. Pure Appl. Math.*, vol. 18, no. 4, pp. 697–715, 1965, doi: 10.1002/cpa.3160180408.

[46]   D. Bjerketvedt, K. Vaagsaether, K. Kristoffersen, A. Mjaavatten, G. Thomas, and R. Bambrey, "Simulation of gas explosions with a Matlab version of the Random Choice Method (RCM)," *http://dx.doi.org/10.1051/jp4:20020290*, vol. 12, Aug. 2002, doi: 10.1051/jp4:20020290.

Appendices

Appendix A. Task description.

Appendix B. Experiment steps.

Appendix C. Python code: Static Pressure Plotting

Appendix D. Python code: Overpressure response in NI and PicoScope.

Appendix E. Python code: Overpressure, shock wave, reflected shock wave plotting, waves velocity, and sampling rate calculation.

Appendix F. Python code: Strain Plotting.

Appendix G. Python code: Overpressure, recorded strain, and simulated strain plotting.

Appendix A. Task Description

FMH606 Master's Thesis

Title: Structural Loads Due to Detonations in Hydrogen Emergency Vent Systems

USN supervisor: Dag Bjerketvedt and Magne Bratland

External partner: Equinor

Task Background: Emergency relief venting systems are standard safety devices in the process industry. If critical events occur, like high pressures, the relief venting systems will act as a safety barrier and rapidly vent the gas. An explosive mixture may occur in the relief venting systems of the hydrogen electrolyzer unit. Therefore, the venting system (mainly safety valves, rupture disc, and pipe) must withstand internal explosion loads to prevent uncontrolled releases. The load will depend on the flame propagation mode in an explosion event. The most devastating event is a transition to detonation. The key questions are, therefore: i) Can the gas detonate? and ii) What is the structural response to detonation?

Task description:

- Review the literature on the transition from deflagration to detonations (DDT) and propagation of detonations in pipes and the associated loads.
- Use RCM (Random Choice Method) to simulate the structural loads in pipes subjected to DDT and detonations.
- Perform an experimental study of DDT in pipes containing hydrogen and air. Use strain gauges and pressure transducers to collect relevant data focusing on pressure records.

Student category: EET or PT students. The tasks are well-tailored for students with a B.Sc. in mechanical engineering.

Is the task suitable for online students (not present at the campus) No

Practical arrangements: Experiments in USN-laboratory Porsgrunn

Supervision:
As a general rule, the student is entitled to 15-20 hours of supervision. This includes necessary time for the supervisor to prepare for supervision meetings (reading material to be discussed, etc).

Signatures:

Supervisor (date and signature): 1/2 - 2024   *Dag Bjerketvedt*

Student (write clearly in all capitalized letters): RUKON AHMED EIMON
Student (date and signature): 01- 02- 24   *RAons*

Appendix B. Experiment Steps

Checklist and results matrix for explosion channel experiments.

Date: 14.03.24   Project Number: 24-SEI-P104

01 – Protection gear	✓	07 – Place ventilation hood accordingly	✓
02 – Check fire extinguisher	✓	08 – Prepare gas cylinder(s)	✓
03 – Start ventilation	✓	09 – Prepare air compressor	✓
04 – Turn off automatic door opener	✓	10 – Start all sensors	✓
05 – Turn on warning light	✓	11 – Start data acquisition systems	✓
06 – Check state of explosion channel	✓		

Note: 79   80   81   82   83

Name of experiment	T00011	T00012	T00013	T00014	T00015
Time	12'50	13.10	13.30	13.50	2.10
Type of fuel	H2	H2	H2	H2	H2
Concentration target	0.6	0.6	0.8	0.8	1.0
Open outlet valve	✓	✓	✓	✓	✓
Close inlet valve	✓	✓	✓	✓	✓
Air mass flow meter 1 (Target)	287	287	287	287	287
Fuel mass flow meter 2 (Target)	18.05	18.05	24.07	24.07	30
Start mass flow acquisition	✓	✓	✓	✓	✓
Start timer (30 s)	✓	✓	✓	✓	✓
Start timer (5 min)	✓	✓	✓	✓	✓
Open inlet valve	✓	✓	✓	✓	✓
Start air flow	✓	✓	✓	✓	✓
Adjust Air flow meter 1	✓	✓	✓	✓	✓
Start fuel flow	✓	✓	✓	✓	✓
Adjust fuel flow meter 2	✓	✓	✓	✓	
Start timer (60 s)	✓	✓	✓	✓	✓
Prepare pressure sensors	✓	✓	✓	✓	✓
Save data in oscilloscope	✓	✓	✓	✓	✓
Close inlet valve	✓	✓	✓	✓	✓
Check for zero H2 flows		✓		✓	✓
Close outlet valve	✓	✓	✓	✓	✓
Check Pico running	✓	✓	✓	✓	✓
Check strain + accelerometer	✓	✓	✓	✓	✓
Ignite mixture	✓	✓	✓	✓	✓
Ignition (Yes/No)	✓	✓	✓		
Open outlet valve	✓	✓	✓	✓	✓
Open inlet valve	✓	✓	✓	✓	✓
Flush system (5 min)	✓	✓	✓	✓	✓
Save all data	✓	✓	✓	✓	✓
DDT (Yes/No)	✗	✗	✓	✓	✓
Close inlet valve	✓	✓	✓	✓	✓

01 – Shut down compressor and gas supply	✓	06 – Stop ventilation	✓
02 – Shut down computers	✓	07 – Turn off warning light	✓
03 – Turn off sensors and data acquisition systems	✓	08 – Turn on automatic door opener	✓

Remember to write any comments or remarks in the logbook

Appendix C. Python code: Static Pressure Plotting

```python
"""
Created on Thu Feb 29 13:49:52 2024

@author: Rukon Ahmed Eimon
"""

import pandas as pd
import numpy as np
import matplotlib.pyplot as plt
from scipy.signal import savgol_filter

# Define the file path
file_path = "static_05.csv"

# Open the file in read mode
with open(file_path, "r") as file:
    data = file.readlines()

firstline = data[0]

# Skip the header line
data = data[1:]

# Split each line into a list of values
data = [line.strip().split(";") for line in data]

# Create a list of column names from the first line
column_names = firstline.strip().split(";")

# Remove the column names from the data
data = data[2:]

# Read the data into a pandas DataFrame
df = pd.DataFrame(data, columns=column_names)

# replace comma with dot
df = df.replace(",", ".", regex=True)

# removing infinities from the dataframe
df = df.replace("âˆž", pd.NA)
df.dropna(inplace=True)

# Convert all columns to numeric data type
df[column_names] = df[column_names].apply(pd.to_numeric)
```

```python
# Subtract the initial value from all columns except 'Time'
for column in df.columns[1:]:  # Assuming the first column is 'Time'
    initial_value = df[column].iloc[0]
    df[column] = df[column] - initial_value

#Scaling and signal filtering
"""Scaling: pressure transducers scaling was set 20 bar per voltage and
1 bar = 0.1 Mpa. Finally multiplied by .25 to cover the maximum within .5m
distance
scale factor = 20*0.1*.25 = 0.5"""

for column in df.columns[1:]:
    if pd.api.types.is_numeric_dtype(df[column]):
        df[column] = df[column] * 20
        #Signal filtering
        df[column] = savgol_filter(df[column], window_length=9, polyorder=1)

obstacle = np.ones_like(df['Time'])

# Plotting
plt.plot(df['Time'], df[df.columns[1]], label='P0')
plt.plot(df['Time'], df[df.columns[2]], label='P1')
plt.plot(df['Time'], df[df.columns[3]], label='P2')
plt.plot(df['Time'], df[df.columns[4]], label='P3(static one)')

plt.title('Static overpressure vs time ')
plt.xlabel('Time (s)')
plt.xlim(0, 60)
#plt.ylim(0, 4)
plt.ylabel('Overpressure (bar)')
plt.legend(loc='upper right')
plt.show()
```

Appendix D. Python code: Overpressure response in NI and PicoScope.

```python
"""
Created on Mon Mar 25 22:00:58 2024
@author: Rukon Ahmed Eimon
"""
import pandas as pd
import matplotlib.pyplot as plt
from scipy.signal import savgol_filter

# Load and process data from Excel
file_path = '32_Eimon.xlsx'
df_excel = pd.read_excel(file_path)
time = 1000 * df_excel['Time']
pressure = 0.1 * df_excel['Pressure']
initial_pressure = pressure.iloc[0]  # Get the initial pressure value
pressure = pressure - initial_pressure # Subtract the initial pressure from
the pressure column

# Apply Savitzky-Golay filter
window_size = 9
poly_order = 1
pressure_smooth = savgol_filter(pressure, window_size, poly_order)

# Load and process data from CSV
file_path = "24_SEi_P104_T00032NI_Pico.csv"
with open(file_path, "r") as file:
    data = file.readlines()

firstline = data[0]
data = data[1:]  # Skip the header line
data = [line.strip().split(";") for line in data]

# Create a list of column names from the first line
column_names = firstline.strip().split(";")

# Remove the column names from the data
data = data[2:]
df_csv = pd.DataFrame(data, columns=column_names)
df_csv = df_csv.replace(",", ".", regex=True)  # Replace comma with dot
df_csv = df_csv.replace("âˆž", pd.NA)  # Removing infinities from the
dataframe
df_csv.dropna(inplace=True)
df_csv[column_names] = df_csv[column_names].apply(pd.to_numeric)

# Subtract the first data of every column from the corresponding column
```

```python
first_values_csv = df_csv.iloc[0, 1:]
df_csv.iloc[:, 1:] = df_csv.iloc[:, 1:].sub(first_values_csv)

# Apply Savitzky-Golay filter on a specific column
df_csv[df_csv.columns[4]] = savgol_filter(df_csv[df_csv.columns[4]],
window_size, poly_order)

# Plotting
plt.plot(df_csv['Time'], 2 * df_csv[df_csv.columns[4]], label='Picoscope',
color='green')
plt.plot(time, pressure_smooth, color='blue', label='NI')
plt.xlim(32, 48)
plt.legend(loc='upper right')
plt.title('Pressure response at P3, ER-0.8, Filter window size 9, polyorder
1')
plt.xlabel('Time (ms)')
plt.ylabel('Overpressure (MPa)')
plt.show()
```

Appendix E. Python code: Overpressure, shock wave, reflected shock wave plotting, waves velocity, and sampling rate calculation:

```python
"""
Created on Mon Mar 4 22:00:58 2024

@author: Rukon Ahmed Eimon
"""
import pandas as pd
import numpy as np
import matplotlib.pyplot as plt
from scipy.signal import savgol_filter

# Define the file path
file_path = "24_SEi_P104_T00016.csv"

# Open the file in read mode
with open(file_path, "r") as file:
    data = file.readlines()

firstline = data[0]
data = data[1:] # Skip the header line
# Split each line into a list of values
data = [line.strip().split(";") for line in data]
# Create a list of column names from the first line
column_names = firstline.strip().split(";")
data = data[2:] # Remove the column names from the data
# Read the data into a pandas DataFrame
df = pd.DataFrame(data, columns=column_names)
df = df.replace(",", ".", regex=True) # replace comma with dot

# removing infinities from the dataframe
df = df.replace("âˆž", pd.NA)
df.dropna(inplace=True)
# Convert all columns to numeric data type
df[column_names] = df[column_names].apply(pd.to_numeric)
# Subtract the first data of every column from the corresponding column
first_values = df.iloc[0, 1:]
df.iloc[:, 1:] = df.iloc[:, 1:].sub(first_values)

#Scaling and signal filtering
"""Scaling: pressure transducers scaling was set 20 bar per voltage and
1 bar = 0.1 Mpa. Finally multiplied by .25 to cover the maximum within .5m
distance.
scale factor = 20*0.1*.25 = 0.5"""

for column in df.columns[1:]:
    if pd.api.types.is_numeric_dtype(df[column]):
```

```python
        df[column] = df[column] * 0.5
        df[column] = savgol_filter(df[column], window_length=9, polyorder=1)

#The following need to be read from the graph
t0 = 20.320 # Ignition time
t1 = 24.462 # shock wave passing time at P1
t3 = 25.4732 # shock wave passing time at P3
t2_ref = 27.3240 # Reflected wave passing time at P2
t0_ref = 28.9283 # Reflected wave passing time at P0

ignition = t0 * np.ones(1000) # Ignition
y = np.linspace(0,4,1000)
obstacle = np.ones_like(df['Time']) # Obstacle
position = np.ones_like(df['Time']) # Position

#sampling rate
sampling_rate = np.round((1000 / ((df['Time'].iloc[1010] -
df['Time'].iloc[10])/ 1000))/1000000)
print(f"Sampling rate: {sampling_rate} MHz")

# Shock wave,Detonation velocity
shock = np.polyfit([t1, t3], [1.5, 3.5], 1)
poly_eq_shock = np.poly1d(shock)
p_end = 4.0
p_det = 1.0
t_end = np.roots(poly_eq_shock - p_end)
t_det = np.roots(poly_eq_shock - p_det)
t_shock = np.zeros(3)
t_shock[0] = t1
t_shock[1] = t3
t_shock[2] = t_end
p_shock = [ 1.5, 3.5, 4.0]
t_shock_dot = np.zeros(2)
t_shock_dot[0] = t_det
t_shock_dot[1] = t1
p_shock_dot = [ 1.0, 1.5]
detonation_velocity = np.round((3.5-1.5)/(t3 - t1)*1000)
print(f"Detonation velocity: {detonation_velocity} m/s")

# Reflected Shock wave,Reflection velocity
t_shock_ref = np.zeros(2)
t_shock_ref[0] = t0_ref
t_shock_ref[1] = t2_ref
p_shock_ref = [0.0, 2.0]
t_shock_ref_dot = np.zeros(2)
t_shock_ref_dot[0] = t2_ref
t_shock_ref_dot[1] = t_end
```

```python
p_shock_ref_dot = [2.0, 4.0]
reflection_velocity = np.round((2.0 - 0.0) / ( t0_ref-t2_ref ) * 1000)
print(f"Reflection velocity: {reflection_velocity} m/s")

# Plotting
plt.plot(df['Time'], 0 + df[df.columns[1]], label='P0')
plt.plot(df['Time'], obstacle, label='Obstacle', linestyle='--',
color='black')
plt.plot(df['Time'], 1.5*position, linestyle='--', color='blue')
plt.plot(df['Time'], 1.5 + df[df.columns[2]], label='P1', color='blue')
plt.plot(df['Time'], 2.0*position, linestyle='--', color='green')
plt.plot(df['Time'], 2.0 + df[df.columns[3]], label='P2', color='green')
plt.plot(df['Time'], 3.5*position, linestyle='--', color='orange')
plt.plot(df['Time'], 3.5 + df[df.columns[4]], label='P3', color='orange')
plt.plot( ignition,y, label='Ignition', linestyle='--', color='red')

plt.plot (t_shock, p_shock, label='Shock wave', color='purple' )
plt.plot (t_shock_dot, p_shock_dot, linestyle='--', color='purple')
plt.plot(t_shock_ref, p_shock_ref, label='Reflected Shock wave',
color='magenta')
plt.plot (t_shock_ref_dot, p_shock_ref_dot, linestyle='--', color='magenta')
plt.title('OverPressure at different position, shock wave, Reflected shock
wave, ER = 1.0')
plt.xlabel('Time (ms)')
plt.xlim(19, 32)
plt.ylim(0, 4)
plt.ylabel('Position + 0.25*overpressure (MPa)')
plt.legend(loc='upper right')
plt.show()
```

Appendix F. Python code: Strain Plotting.

```python
"""
Created on Mon Mar 14 22:23:09 2024

@author: Rukon Ahmed Eimon
"""

import pandas as pd
import matplotlib.pyplot as plt
from scipy.signal import savgol_filter

# Load the Excel file into a pandas DataFrame
file_path = '24_SEi_P104_T00016.xlsx'
df = pd.read_excel(file_path)

first_values = df.iloc[0, 1:]  # Extracting the first data of every column
except the Time column
df.iloc[:, 1:] = df.iloc[:, 1:].sub(first_values)

# Factor is calculated from voltage to strain conversion factor
time = 1000 * df['Time']
strain_a = df['strain_a']*0.762
strain_b = df['strain_b']*0.762
strain_c = df['strain_c']*0.762


plt.plot(time, strain_a, color='orange', label='Axial strain')
plt.plot(time, strain_b, color='magenta', label='Strain at 45 degree between
radial and axial direction')
plt.plot(time, strain_c, color='green', label='Hoop strain')
plt.ylabel('Strain')
plt.xlabel('Time (ms)')

plt.title('Strain Response at 2.0 m Distance, ER = 1.0 (No Filter)')
plt.xlim(24, 27)
plt.legend(loc='upper left')
plt.ylim(-0.0004, 0.0004)
plt.show()
```

Appendix G. Python code: Overpressure, recorded strain, and simulated strain plotting.

```python
"""
Created on Mon Mar 16 18:56:29 2024

@author: Rukon Ahmed Eimon
"""

import pandas as pd
import matplotlib.pyplot as plt

# Load and preprocess Excel data
excel_path = '24_SEi_P104_T00016.xlsx'
df_excel = pd.read_excel(excel_path)
initial_values_excel = df_excel.iloc[0, 1:]
df_excel.iloc[:, 1:] = df_excel.iloc[:, 1:].sub(initial_values_excel)
time_ms = 1000 * df_excel['Time']  # Convert time to ms
strain_a_adjusted = df_excel['strain_a'] * 0.762
strain_b_adjusted = df_excel['strain_b'] * 0.762
strain_c_adjusted = df_excel['strain_c'] * 0.762

# Load and preprocess CSV data
csv_path = "24_SEi_P104_T00016.csv"
df_csv = pd.read_csv(csv_path, delimiter=';', decimal=',', skiprows=1)
df_csv.replace("âˆž", pd.NA, inplace=True)
df_csv.dropna(inplace=True)
df_csv = df_csv.apply(pd.to_numeric, errors='coerce')
initial_values_csv = df_csv.iloc[0, 1:]
df_csv.iloc[:, 1:] = df_csv.iloc[:, 1:].sub(initial_values_csv)

# Calculate scaled pressure and simulate values
pressure_scaled = df_csv.iloc[:, 3] * 2
simulate = 7.43e-5 * pressure_scaled

# Create plot
fig, ax1 = plt.subplots()

# Plot pressure from CSV data
pressure_line, = ax1.plot(df_csv.iloc[:, 0], pressure_scaled, color='blue',
label='Overpressure ')
ax1.set_xlabel('Time (ms)')
ax1.set_ylabel('Overpressure (MPa)')
ax1.tick_params(axis='y')

# Twin axis for strains
ax2 = ax1.twinx()
strain_c_line, = ax2.plot(time_ms , strain_c_adjusted, color='green',
label='Hoop strain from strain gauge')
```

```python
simulate_line, = ax2.plot(df_csv.iloc[:, 0], simulate, color='red',
label='Simulated hoop strain from Pressure')
ax2.set_ylabel('Strain')
ax2.tick_params(axis='y')

# Adjust y-axis limits for better visibility
ax1.set_ylim(bottom=-2)
ax2.set_ylim(bottom=-0.0005)

# Combine legends
lines = [pressure_line, strain_c_line, simulate_line]
labels = [line.get_label() for line in lines]
plt.legend(lines, labels, loc='upper right')

# Configure plot details
plt.title('Strain Response at 2.0 m Distance, ER = 1.0')
plt.xlim(24, 27)
plt.show()
```